

Magic Mode

Investigations of Artificial Stimulation of ULF Waves in the Ionosphere and Magnetosphere

JOHN R. DAVIS, JOHN W. WILLIS, AND EDWIN L. ALTHOUSE

*Electromagnetic Propagation Branch
Communications Sciences Division*

March 12, 1973



**NAVAL RESEARCH LABORATORY
Washington, D.C.**

CONTENTS

Abstract	ii
Problem Status	ii
Authorization	ii
 1. INTRODUCTION	 1
Background	1
Purpose	2
 2. THEORETICAL CONSIDERATIONS AND OBSERVA- TIONS OF NATURAL PHENOMENA	 3
Observed Characteristics of Geomagnetic Micropulsations	3
Theoretical Explanations of Micropulsation Characteristics	4
 3. ARTIFICIAL STIMULATION METHODS	 10
Modification of Lower-Ionosphere Currents	10
Stimulation of Wave-Particle and Wave-Wave Inter- actions in the Magnetosphere	24
 4. EXPERIMENTS PROPOSED AND IN PROGRESS	 28
Apparatus	28
ULF Noise Investigations	32
Ionospheric Chemical Releases	35
Ionospheric-Heating Experiments	38
Stimulation of Wave-Particle Interactions in the Magnetosphere	38
Stimulation of Wave-Wave Interactions in the Magnetosphere	39
 5. SUMMARY AND CONCLUSIONS	 39
 REFERENCES	 41

CONTENTS

Abstract	ii
Problem Status	ii
Authorization	ii
 1. INTRODUCTION	 1
Background	1
Purpose	2
 2. THEORETICAL CONSIDERATIONS AND OBSERVA- TIONS OF NATURAL PHENOMENA	 3
Observed Characteristics of Geomagnetic Micropulsations	3
Theoretical Explanations of Micropulsation Characteristics	4
 3. ARTIFICIAL STIMULATION METHODS	 10
Modification of Lower-Ionosphere Currents	10
Stimulation of Wave-Particle and Wave-Wave Inter- actions in the Magnetosphere	24
 4. EXPERIMENTS PROPOSED AND IN PROGRESS	 28
Apparatus	28
ULF Noise Investigations	32
Ionospheric Chemical Releases	35
Ionospheric-Heating Experiments	38
Stimulation of Wave-Particle Interactions in the Magnetosphere	38
Stimulation of Wave-Wave Interactions in the Magnetosphere	39
 5. SUMMARY AND CONCLUSIONS	 39
REFERENCES	41

MAGIC MODE: INVESTIGATIONS OF ARTIFICIAL STIMULATION OF ULF WAVES IN THE IONOSPHERE AND MAGNETOSPHERE

1. INTRODUCTION

Background

Communication to deeply submerged reception terminals from a land-based command-and-control center is governed, as is any communications system, by an electromagnetic power budget which can be divided roughly into four items:

1. Generated Power
2. Radiation Efficiency
3. Path Losses
4. Noise

Electronic countermeasures are included in noise, and traumatic mechanical countermeasures such as high-altitude nuclear explosions can be included in path losses. It is known that (a) the limits on generation of radio-frequency (RF) power are only weakly dependent on frequency over a rather wide band and (b) atmospheric and galactic noise are only slightly more frequency dependent (except between 1 and 4 kHz, where an increase in attenuation tends to compensate for a substantial decrease in noise over most communication paths of interest). Thus the radiation efficiency and path losses are of greatest consequence for such a system. The former varies roughly as the square of frequency, and the latter vary in some irregular manner that depends on the type of propagation exploited (which may employ means, such as ionospheric ducting, to improve the path loss relative to a spherical-spreading law). The overwhelming contribution to path losses for communication to a deeply submerged receiver is attenuation in sea water, which varies in proportion to the square root of the frequency.

Consideration of all of these items together has resulted in a consensus that a command-and-control communications system for direct electromagnetic transmission from shore to submarines at operational depth must employ the frequency band below about 100 Hz. The SANGUINE system, presently planned to operate between 40 and 80 Hz in the ELF band, is one manifestation of this consensus. Despite the small radiation efficiency of the SANGUINE antenna (about 10^{-4}), path losses over pathlengths of thousands of kilometers are only a few decibels, because the earth-ionosphere waveguide effectively confines nearly all radiated power to within 100 km above the surface of the earth. Total loss in sea water to a 100-m depth is only about 25 dB, whereas at VLF it would exceed 300 dB. The very fact of the low attenuation suffered by ELF waves in the earth-ionosphere waveguide provides substantial security against jamming, inasmuch as a potential jammer enjoys very little advantage from being closer to the receiver than is the transmitter. It may be true that high-altitude nuclear-explosion effects on the lower ionosphere, which is of primary importance for earth-ionosphere waveguide propagation, are so small as to

negate this potential countermeasure as well. It is not altogether clear, however, that such effects are indeed negligible.

An alternative low-data-rate system could conceivably operate at an even lower frequency. For example, at about 0.5 Hz, attenuation in sea water to a depth of 100 m would be only 2.5 dB. A ULF communications system operating at this frequency thus would enjoy an advantage of more than 20 dB over even a SANGUINE system in the important criterion of loss in sea water. For receivers at a 300-m depth, which may well be reasonable for foreseeable submarine technology, this advantage is nearly 70 dB and could easily outweigh any advantage in predetection information bandwidth possessed by the ELF system. However, the matter of radiation efficiency practically precludes the use of conventional radio transmitting methods for a ULF communications system, and such a system could not realistically be conceived as a direct competitor to a SANGUINE-type ELF system.

There are several matters which make a ULF system for information transmission of potential, albeit speculative, interest, and these matters all center around a possibility that unconventional means of power amplification and radiation can supplant the commonly pictured earth-based transmitter and metallic antenna structure. A similar waveguiding principle to that which affords ELF waves their low attenuation rate in the earth-ionosphere waveguide also may be exploited for ULF propagation. If a mechanism for ULF wave generation can be devised which has a radiation efficiency no *worse* than the 10^{-7} to 10^{-8} , which the frequency-squared proportionality would suggest is a practical limit at ULF for conventional means of RF radiation, then a communications system at this low-frequency extreme would be competitive with an ELF system for communicating with receivers at depths of several hundred meters. As will be evident from later discussion, the wave-generation mechanisms currently under consideration are not limited by any inherent efficiency parameter such as that quoted above, but so little is known about them that achievable radiation efficiencies could range as well below those values as above them.

Purpose

It is the purpose of this report to review the present knowledge of ULF generation and propagation mechanisms with the intent of identifying those areas of investigation which must be explored further before an intelligent assessment can be made of the suitability of the ULF band for command-and-control communications. The material which appears in Part 2 of this report is intended to show the extent to which measurements of natural phenomena in the ULF band, augmented by theory, suggest that wave generation and amplification mechanisms are operative *naturally* in the magnetosphere and may be available for artificial exploitation. This review material is drawn largely from the open scientific literature.

Subsequent material in this report is directed toward describing investigations underway at NRL in search of a means of artificially generating ULF waves and in quest of further knowledge regarding their propagation in the magnetosphere and ionosphere. Part 3 of this report contains descriptions of the most attractive methods by which ULF waves may be stimulated artificially. These methods are divided into two types: techniques for modifying the dynamo currents which flow naturally in the lower ionosphere and techniques for bringing about and controlling interactions between electromagnetic waves and the magnetospheric plasma. The former type of stimulation method appears to be the more attractive of the two, and we therefore describe in detail a number of experiments which

can be conducted to test the thesis that ULF waves can be launched in such a manner. One of these experiments involves the injection of ionized gases into the ionosphere, thus modifying the electrical conductivity of that region and so altering locally the magnitude and direction of the ionospheric dynamo currents. Other experiments use ionospheric heating produced by powerful, earth-based RF transmitters in the high-frequency band to bring about changes in ionospheric conductivity or to create perturbed electric fields in the ionosphere, either of which may lead to modification of the flowing dynamo currents.

Methods of bringing about wave-particle and wave-wave interactions in the magnetosphere are treated briefly and qualitatively. They have been discussed superficially in the open scientific literature, but no experimental evidence exists on which reliable quantitative estimates of their effectiveness as ULF wave-generation techniques can be based.

Part 4 of this report contains a discussion of the experiments which have been conducted by NRL, as well as those which are planned. Inasmuch as these experiments are in a preliminary stage, only a very limited body of evidence has been gathered. Part 4 is intended only as an interim status report.

Part 5 is a summary of the principal points we hope to have made in this report—namely a description of the most attractive means for attempting artificial stimulation of ULF waves and a description of the experiments planned to test these means.

2. THEORETICAL CONSIDERATIONS AND OBSERVATIONS OF NATURAL PHENOMENA

Observed Characteristics of Geomagnetic Micropulsations

Knowledge of the mechanisms by which naturally occurring ULF waves are generated, most of which operate in the near-equatorial magnetosphere at a distance of several earth radii or in the auroral ionosphere, is limited to that which can be discerned from observations of geomagnetic micropulsations. The same is true of the parameters that describe the propagation of these waves in the magnetosphere and their impingement on the ionosphere. It is not surprising that this circumstance has developed. In the ELF band, for example, the occurrence of Schumann resonances and the behavior of discrete atmospheric waves were responsible for discovery of the earth-ionosphere waveguide on whose existence a SANGUINE communications system is dependent. It was not until the propagation characteristics of ELF waves were reasonably well understood by observations of natural phenomena and theoretical modeling of the earth-ionosphere waveguide that the considerable expense of artificial-transmission experiments became worthwhile. The same is true of ULF wave propagation.

Reliance on natural phenomena to investigate propagation in a medium so inhomogeneous, anisotropic, and fluctuating as the ionosphere has its dangers, of course. Just as the development of an ELF communications system has evolved through several iterations of the observation/theoretical-development/experiment-design cycle and will probably undergo several more iterations, the study of ULF generation and propagation phenomena must proceed with present knowledge of observed natural phenomena, supplemented by theory, as only the basis for an experiment design leading to further such iterations. At present this knowledge is dependent on fortuitous natural stimuli; it is planned that future efforts should include efforts at artificial stimulus together with intensified study of natural events.

Geomagnetic micropulsations in the frequency band of interest, nominally 0.5 to 5 Hz, are of two types and are designated by international convention as Pc 1 (Pulsations, continuous, Type 1) and Pi 1 (Pulsations, irregular, Type 1). The numeral one simply indicates the specific frequency range into which these phenomena fall, and this value includes the band of interest for this investigation. The designation "continuous" refers to a quality of Pc 1 micropulsations which is of great importance for studying generation and amplification mechanisms—their appearance as an extended pulse train, most often of a duration of about a half hour, of relatively-narrow-bandwidth (usually about 10 to 20 percent bandwidth) wave packets of a few tens of seconds length, separated by intervals of several seconds (1,2). The designation "irregular" pertains to single pulse-like emissions in the same general frequency band which do not appear in repetitive sequences and which are normally of much broader bandwidth. There are in addition to these two classifications a number of subclasses whose individual characteristics have helped unravel the knotty physics of the generation and propagation of ULF waves but which are unnecessary detail for our purposes.

The prominent features of Pc 1 micropulsations, in addition to the repetitive, narrow-band pulse sequence in which they appear, are as follows:

- They occur alternately at magnetically conjugate stations, indicating that they propagate back and forth along the geomagnetic field lines joining the stations (1,2).
- They often commence at low amplitude, grow in tens of minutes to a maximum amplitude which is maintained over several pulse periods, and gradually decay somewhat more slowly (3).
- They generally display a spectral appearance which suggests a dispersive type of propagation in the magnetosphere (2). (However, in some subclasses, presumably generated by a different source mechanism, they do not (1,4).)
- They are detected most strongly in the auroral regions (5).
- They propagate to lower latitudes with a group velocity of several hundred km/s (6,7).
- They undergo in this propagation an attenuation of 1 to 2 dB/1000km in the darkened hemisphere and of considerably greater magnitude in the sunlit hemisphere (8).

Pi 1 micropulsations display some of these same characteristics but are of interest primarily because they are found to coincide with the precipitation of charged particles and X-rays into the auroral ionosphere (1,2,9). Hence, they may indicate that a low-altitude ionospheric source mechanism (in the case of auroral phenomena, at about 100 km) may possibly exist.

Theoretical Explanations of Micropulsation Characteristics

The occurrence of Pc 1 and Pi 1 micropulsations has been a matter of scientific curiosity for several years, and theoretical efforts have been successful in providing an explanation for most of their characteristics. It is now widely accepted that under some

circumstances the energy spectrum of trapped protons in the magnetosphere permits energy to be transferred from the trapped particles to magnetohydrodynamic (MHD) waves of the proper frequency, phase velocity, and polarization (10-13). This circumstance leads to the characterization of the trapped-proton belt as an amplifier and explains the observed characteristic frequencies, bandwidths, repetition rates, and polarization of Pc 1 micropulsations. It also predicts that Pc 1 micropulsations will be concentrated in and near the auroral regions. A theory of magnetoionic ducting has also been developed which requires ULF waves to impinge on the ionosphere from the magnetospheric amplifier region and to be transformed into a different form of MHD wave which is suitable for propagation over the surface of the earth in a spherical duct centered on the ionospheric F region. This theory explains the polarization, group velocities, and low attenuation rates observed in Pc 1 and Pi 1 micropulsations detected at temperate and equatorial latitudes (7,8,14,15,16).

This combination of observations of natural phenomena with theoretical explanation of the observed micropulsation characteristics has permitted a crude, schematic picture of ULF wave amplification and propagation to be formed. Figure 1 is a sketch of the earth, ionosphere, and magnetosphere in which the prominent features of this process are indicated. The closed circle at the left represents the earth, and the stippled ring encircling it illustrates the ionospheric duct described previously. The boundaries of the duct are nominally 100 and 2000 km above the surface of the earth. The wedge-shaped, cross-hatched region is a rough indication of that region of the magnetosphere in which protons, of the proper energy spectrum to interact with ULF waves and amplify them, are trapped. The eccentric circles passing between the northern and southern hemispheres of the earth are a schematic representation of the magnetic field of the earth. The labels $L = 2$ to $L = 9$, which appear in the equatorial plane, represent parameters of a geomagnetic coordinate system and indicate the distance in earth radii of each geomagnetic field line from the center of the earth in the equatorial plane. The trapped-proton region extends from about $L = 2.6$ to $L = 6$.

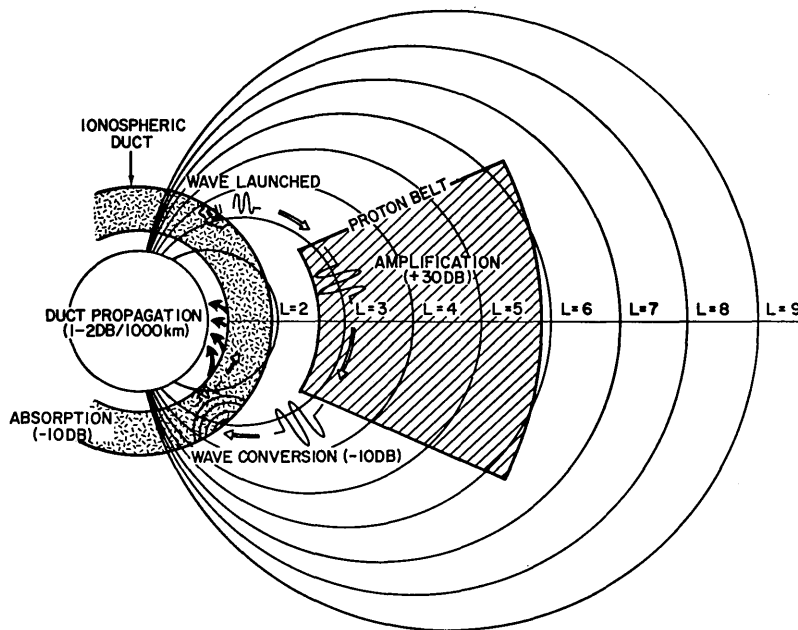


Fig. 1—Schematic representation of the earth, ionosphere, and magnetosphere with magnetospheric proton-belt amplification

Without specifying, for the meantime, the means by which a ULF wave is generated, let us suppose that such a wave is launched in an appropriate MHD mode from the ionosphere in the northern auroral zone. The mode of interest is a left-hand-polarized, slow Alfvén wave, because this particular type of MHD wave will be guided by the magnetic field and channeled into the proton belt (17,18). In Fig. 1 this channeling is indicated as taking place along the $L = 3$ contour. On entering the proton belt, the ULF wave will interact with the resident protons by a mechanism which is reminiscent of a traveling-wave-tube amplifier. That is, for a wave whose sense of polarization is the same as the direction in which the protons are spiraling around the direction of the magnetic field and whose frequency (when doppler shifted) equals the frequency of particle rotation, a transfer of energy can take place from the gyrating particles to the wave. This process is analogous to a traveling-wave tube in which the spiraling-proton beam forms a slow-wave structure. As indicated in Fig. 1, an amplification limit of about 30 dB is probable (11,12). This value is consistent with the results of observations of natural micropulsations and indicates that there is not an inexhaustible supply of protons with the proper energy and spiral pitch angle for coupling with the ULF wave (12).

On emerging from the proton belt, the amplified ULF wave continues to be guided by the magnetic field and impinges on the ionosphere. Figure 1 shows this event taking place in the southern hemisphere.

The left-hand-polarized wave is partially absorbed in the lower ionosphere (19). It can be detected in a small region on the earth directly below its point of impingement on the ionosphere, due to the quasi-evanescent wave fields which penetrate to and below the surface of the earth (20,21). However, a process which occurs within the ionospheric E region *above* the altitude of high absorption for these waves permits further low-loss propagation to proceed away from the ionospheric source region. In the ionospheric E region, a mode-conversion process takes place in which the left-hand-polarized, slow Alfvén wave is converted to a (locally-right-hand-polarized) fast Alfvén wave (19). The latter mode suffers considerable absorption when passing downward through the lower ionosphere but, more importantly, is *ducted* horizontally by the ionosphere above this absorbing region. As is indicated in Fig. 1, the wave-conversion process entails a loss of about 10 dB (19). This value is consistent with observations of natural phenomena and accounts for energy which is coupled into other modes as well as energy which is reflected back along the direction of the magnetic field toward the proton belt (where, incidentally, it can be further amplified and in the case of Pc 1 micropulsations gives rise to subsequent pulses in the long train of wave packets which is typically observed). We also have indicated in Fig. 1 an absorption of about 10 dB in the lower ionosphere. This figure, which also is motivated by observations of natural phenomena (8), accounts for collision-related losses in the ionospheric D region. It may be an overestimate for the darkened hemisphere, where some measurements suggest that there is very little absorption in the nighttime D region.

Finally, there occurs the process of ducted propagation which, as indicated in Fig. 1, takes place with an attenuation rate as low as 1 dB/1000km (8). It is likely that so low an attenuation rate will hold only for an undisturbed ionosphere in darkness. In the sunlit hemisphere, an attenuation rate of 3 to 5 dB/1000 km is probably more realistic (8). We have sketched a series of solid arrows at the bottom of the duct, indicating that energy leaks from the lower boundary of the duct to points on and beneath the surface of the earth. This energy reaches the earth by means of the quasi-evanescent wave fields which extend below the duct boundary. Once again, observations of natural phenomena, supplemented by a considerable theoretical effort, have served as the basis for these estimates of attenuation rate.

Two aspects of this amplification/propagation process merit further treatment.

- The specific ducting mechanism.
- The regions of the earth accessible to waves incident from the magnetosphere.

The ionospheric electron density normally rises from near zero at an altitude of 60 km or so to a maximum of 10^5 to 10^6 cm^{-3} at the F-region peak in the altitude range of 200 to 400 km and then gradually decays to a value of 100 cm^{-3} or so at the plasmopause several thousand kilometers from the earth. The refractive index, correspondingly, reaches a maximum (for frequencies in the ULF range) at the F-region peak, and this behavior is responsible for the formation of a duct centered on that altitude. In the case of ULF waves, the operative mechanism can be understood more directly as being a consequence of a minimum in the Alfvén velocity, which is inversely proportional to the square root of ion mass density. The Alfvén-wave duct which is formed in the ionosphere is illustrated by the typical electron-density profile and associated Alfvén-velocity profile of Fig. 2. Its upper and lower boundaries are roughly 2000 km and 100 km respectively. It is the penetration of the wave to the relatively dense region 100 km and below which is responsible for the 10-dB absorption indicated in Fig. 1; the curve in this region on Fig. 2 is typical of darkened conditions, for which overall absorption is small. Under sunlit conditions, the electron-density curve would extend to 10^4 cm^{-3} or even higher densities at the 100-km altitude, causing the wave to descend into a region of higher collisions and leading to a substantial increase in absorption.

It was indicated in Fig. 1 that the geomagnetic L coordinates 2.6 and 6 bound the latitudes from which earth-launched, left-hand-polarized ULF waves can reach the proton belt and there be amplified by ion cyclotron interaction with the resident protons. The regions on the surface of the earth which fall within these boundaries are indicated in

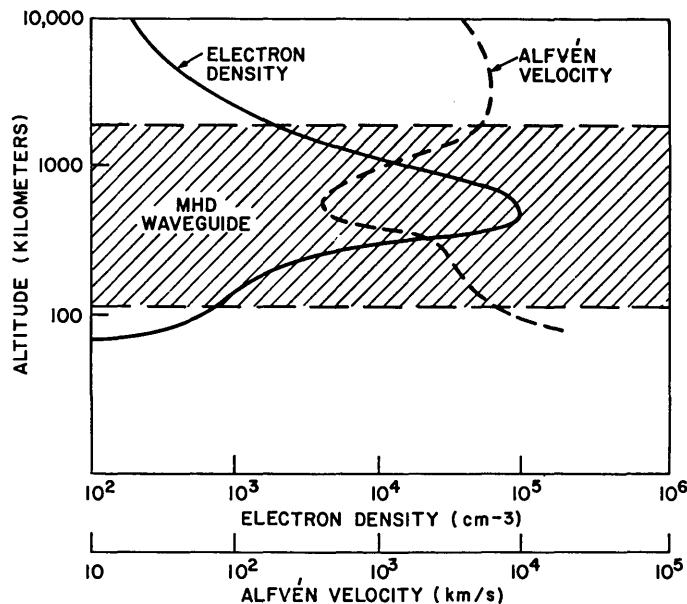


Fig. 2—Typical ionospheric electron-density and Alfvén-velocity profiles for the darkened hemisphere. The Alfvén or magneto-hydrodynamic (MHD) waveguide is shown cross-hatched.

Fig. 3. In the northern hemisphere this "micropulsation generation zone" passes over Alaska and the northern Soviet Union. In the southern hemisphere it crosses land only in the Antarctic, the southern tip of Australia, and the south island of New Zealand.

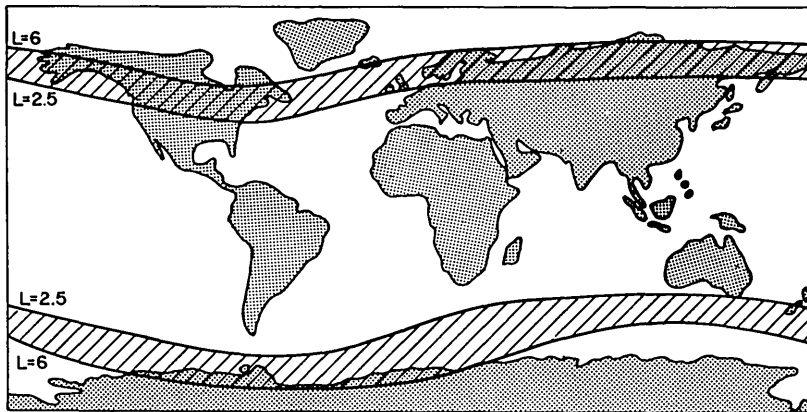


Fig. 3—Regions on the earth directly accessible to ULF waves generated or amplified in the magnetospheric proton belt

It should be recalled that these two areas represent only the regions of the ionosphere which are *directly* accessible to ULF waves arriving from the "magnetospheric amplifier." Ducted waves in the ionospheric waveguide can propagate in all directions from these regions, for several thousand kilometers under suitable conditions, with very low losses. Micropulsations which arrive at the indicated latitudes from the magnetosphere are routinely detected at temperate latitudes, for example, and are often received at equatorial stations. It also should be borne in mind that access to the ionospheric waveguide is not necessarily restricted to the latitude band indicated in Fig. 3. Artificial means of ULF wave generation could presumably be effective in launching waves at any geographical position if wave fields of adequate magnitude could be created. The micropulsation-generation bands represent only the regions in which ULF waves from the magnetospheric amplifier are injected into the duct.

If an artificial ULF wave-generation mechanism is to take advantage of natural amplification processes in the magnetosphere, the resulting signals will be coupled into the ionospheric waveguide in the indicated regions and will propagate to other latitudes in the waveguide. The material to be presented in Parts 3 and 4 of this report concerns a series of experimental investigations which are intended to explore the possibility of artificially generating ULF waves both within the micropulsation-generation bands (hence exploiting the magnetospheric amplifier) and at temperate latitudes (simply relying on the low attenuation of the ducted waves for achieving useful transmission ranges).

To this point the matter of ULF wave sources has been ignored, and for a very important reason. Whereas a good deal is known about the propagation modes within the magnetosphere and within the ionospheric duct and though the magnetospheric amplification process is reasonably well understood to a first approximation, very little is known of the ultimate wave sources. We mentioned previously that Pi 1 waves display a strong association with the bombardment of the auroral-zone ionosphere by solar charged-particle and X-ray fluxes. Indeed, the complex temporal structure of Pi 1 micropulsations is highly correlated with the variation of certain types of auroral emission intensity and with the

fine details of charged-particle and solar X-ray fluxes sensed on the earth and by satellites. It is conjectured that this type of ULF wave arises when the lower-ionosphere electrical conductivity is, in effect, modulated by the impact of these energetic particles and X-rays. This modulation of the conductivity, together with existing atmospheric electric fields, leads to changes in the electric currents which flow in the lower E region and hence to fluctuations of the magnetic field. If this supposition is correct, then an artificial ULF wave-generation method might consist simply of a device which can modulate the ionospheric current in the lower E region. The desired modulation could be achieved either by (a) changing the charged-particle population, as is suspected occurs in the auroral region during the excitation of Pi 1 micropulsations, (b) modulating the electric fields while keeping the conductivity constant, such as can be achieved with an ionospheric interaction process leading to the development of charge-separation fields, or (c) modulating the current directly by introducing charged-particle beams in the approximate region.

The source for Pc 1 micropulsations also is poorly understood. One common hypothesis is that they occur spontaneously in the proton belt when the particle energy spectrum is appropriate (4,12). An analogy with a traveling-wave-tube (or, more properly, a backward-wave) oscillator is, of course, tempting; indeed, any amplifier when properly terminated can act as an oscillator, and so such an analogy in this case is quite a legitimate one. For want of a more concrete explanation, we will assume that Pc 1 micropulsations represent a spontaneous response of the magnetospheric proton belt to some unspecified noise-like excitation; we will assume that a potential artificial source could operate by creating in the charged-particle population a condition of latent instability similar to that which presumably exists when Pc 1 micropulsations occur.

A number of workers have attempted to model the proton energy spectrum which would be required to afford this type of behavior, and comparison of these models with satellite measurements indicates that the required conditions may be present rather frequently (11-13). Furthermore, theoretical exercises have suggested that injection of a reasonable amount of an ionized gas into the proton belt could artificially create the necessary conditions (22). Consequently, in addition to those artificial mechanisms which would modify the parameters of the lower ionosphere, we must consider those which would modify the magnetospheric amplifier.

There is, finally, a possibility that coupling of energy into an MHD wave in the ULF band could take place by a three-wave process, such as occurs in a parametric amplifier or laser (23,24). It is suggested that under suitable conditions energy from two high-intensity VLF wave fields could be coupled into a ULF wave whose frequency and wave vector is properly related to the VLF pair. The mechanism for bringing about this three-wave process is a matter for conjecture, but certain circumstances make it of interest:

- A magnetospheric amplification process analogous to that we have described previously for ULF waves also occurs at VLF and is capable of far more than the nominal 30-dB amplification we have indicated for ULF waves.
- VLF transmitters of considerable power are available and could be appropriately modulated to yield the desired ULF difference frequency. Provided VLF power can be directed from the earth into the correct region of the magnetosphere, the relatively weak VLF waves then could undergo amplification and reach the intensity which is essential to trigger the three-wave process. The resultant ULF wave would then be detected on the earth after the expected further amplification, propagation along the magnetic field to the ionosphere, and ducting in the

ionospheric waveguide. It should be mentioned, incidentally, that some experimental data suggest that atmospherics may be a cause for Pc 1 micropulsations under certain circumstances (25). If the mechanism by which the transfer of energy from the lightning stroke in the atmosphere to the proton belt where the micropulsations are generated is, as might be suspected, a VLF whistler wave, then the three-wave interaction we have suggested is possibly the means by which the energy is coupled into the ULF wave from the whistler.

3. ARTIFICIAL STIMULATION METHODS

Modification of Lower-Ionosphere Currents

Among the possible means by which the lower-ionosphere currents might be modified artificially, the most direct method would involve deposition of an ionized gas into an appropriate volume of the E region. It is important that such an experiment take place at an altitude where strong background electric currents flow, thereby providing the means of coupling to the geomagnetic field. These currents flow in the region between 100 and 140 km, where the electrical conductivity tensor is anisotropic. At these altitudes the Hall and Pedersen conductivities cause a maximum to appear in the transverse conductivity component (that component of the conductivity tensor which relates to current flowing perpendicular to the direction of the magnetic field and which, for temperate latitudes, is largely horizontal). The current which flows in this region is the familiar ionospheric dynamo current, and it undergoes a relatively regular diurnal cycle, with peaks in mid-morning and mid-afternoon (in opposite directions) and with nulls at noon and at night. For a given percentage change in electrical conductivity such as might be achieved by an ionospheric chemical release using an ionizable gaseous material, the most attractive times of day for an experiment would be the times of maximum overhead current flow at the launch site. These currents are of greater magnitude in the summer season at temperate latitudes than at other times of the year, so such an experiment should be conducted as near mid-summer as possible.

Two chemical materials and deposition methods are available. Barium metal can be vaporized in a thermite reaction and emitted through a nozzle into the ionosphere. A relatively large fraction (a few percent) of the total payload weight will be photoionized by the sun with a time constant of some tens of seconds. In the 100- to 140-km interval, however, an oxide is formed quite rapidly by the neutral barium, and a very low ion density results (26). Furthermore, this relatively-low-energy release mechanism would result in a barium cloud which would remain in a rather small volume, particularly if released near the lower extreme of the altitude interval.

A second method of plasma-cloud deposition involves detonation of a mixture of a cesium salt and a high explosive (HEX). Although a much smaller fraction of the cesium payload is ionized in this reaction (much less than 1%) than results from the vented-barium method, it possesses a number of important advantages: (a) Cesium is thermally ionized in the detonation process, and hence a very large "pulse" of ions is available immediately (27). The effect on the ambient currents thus should be visible as a large transient and is less likely to be confused with the normal magnetic-field fluctuations which occur regularly with periods of tens of seconds. This feature is particularly important, inasmuch as the sensing devices which are most sensitive in the frequency range of interest (0.5 to 5 Hz) are induction devices. They are thus sensitive to the *rate of change* of the magnetic field, and a method which maximizes the rate at which plasma interaction with the geomagnetic

field takes place is most attractive. (b) The cesium does not form an ionic oxide readily, and a cloud of cesium ions emitted into the E region will remain ionized for many tens of minutes (28). (c) The energy imparted to the cesium cloud in the explosion propels the outer boundaries to a large distance, and hence a large volume of the ionosphere is affected (29); the speed with which the charged spherical volume expands enhances the interaction of the plasma cloud with the constraining background magnetic field. (d) Finally, and perhaps fortuitously, the hydrodynamic time scale of the lower E region is well suited to the electromagnetic time scale of interest (29). That is, the thermodynamic environment in the altitude region of 100 to 140 km in which a detonation of several kilograms of cesium salt plus high explosive would occur imposes a characteristic time scale on the expanding plasma cloud which falls within the frequency band of interest. The plasma cloud expands and undergoes reverberation over time scales of a few tenths of seconds to several seconds, depending on altitude. Consequently, it would be expected that the product of the interaction between the plasma cloud and the ambient currents would be characterized by a wave spectrum centered precisely in the frequency band of interest.

Figure 4 is a sketch of such an experiment. The stippled band represents the ionospheric dynamo region at 100- to 140-km altitude. Shown schematically are three geomagnetic field lines passing through the ionosphere and forming an orthogonal set of axes in geomagnetic coordinates where they intersect the ground (they define north-south and east-west geomagnetic planar surfaces). A rocket conveying the cesium salt and high explosive (in this case, cesium nitrate and TNT in a payload of 140- to 200-lb net weight) is launched from the ground and detonated in the dynamo region. Disturbance current vectors j are shown emanating from the plasma-cloud region, and these disturbance currents give rise to geomagnetic fluctuations ΔB which can be detected on the ground by suitable sensors. In the experimental configuration envisioned, sensors can be placed both directly beneath the burst region and away from it in both the north-south and east-west planes. Thus the source field near the burst point and wave components traveling horizontally in the directions of the orthogonal axes can be detected.

A simple calculation can be performed to give a rough indication of the degree to which the local dynamo current might be perturbed by a plasma-cloud release. Figure 5 is

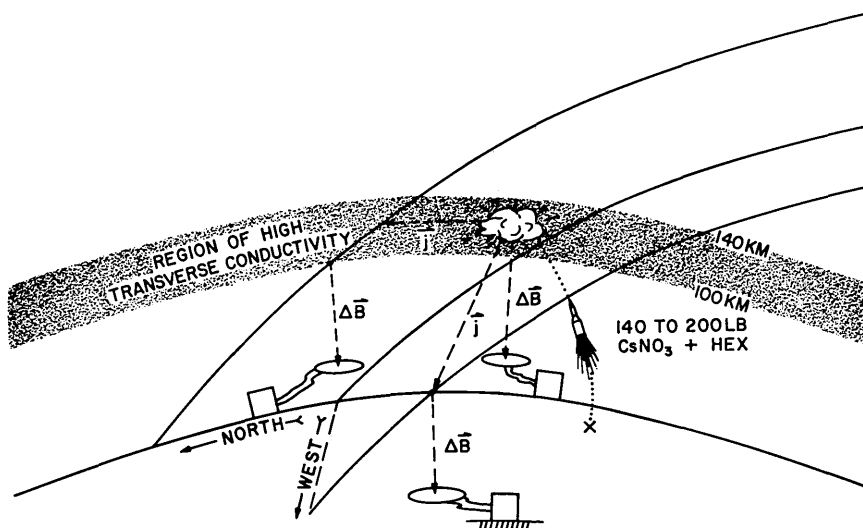


Fig. 4—Sensor network and launch geometry for an experiment to investigate modulation of lower ionospheric conductivity by cesium-plasma-cloud deposition

a sketch of a cylindrical plasma volume with its axis of symmetry along the direction of the background magnetic field B_0 taken to be the negative z direction (to correspond to the northern hemisphere) in a Cartesian coordinate system. For the purposes of this calculation the magnetic field will be taken to be vertical, and the disturbed region is assumed to be unbounded in that direction. An angle α in the horizontal plane will be defined as

$$\alpha = \tan^{-1} \frac{\sigma_2}{\sigma_1} ,$$

where σ_1 and σ_2 are the local Pedersen and Hall conductivities respectively. This angle represents the angular difference between the direction of the background horizontal electric-field component E_0 and the direction of flow of current j_0 . Let E_0 be directed at an angle α from the x axis (so the current will flow in the x direction, for convenience). We consider the perturbed current j' due to a total charged-particle density N' in the plasma cylinder of radius a , which is immersed in an ambient plasma of density N . For an equilibrium case (30), the perturbed current j' is limited by the polarization electric field E_p , which appears across the plasma cloud and is due to charge separation driven by the ambient electric field E_0 . We are concerned here with the transient case, which can be conceived as taking place in two stages. Figure 6 indicates the processes with which we are concerned. Beginning at t_0 , an explosion takes place in which both charged and neutral particles are driven by the thermodynamics of the explosion to form a nominally spherical ionized cloud in pressure equilibrium with the environment. At time t_1 the ionized cloud begins to experience charge separation due to E_0 and continues under this influence for approximately the interval in which a charged particle drifts across the cloud. At time t_2 the polarization electric field E_p has formed across the cloud, and for large N'/N this field limits the perturbed current in the x direction to approximately the value of the undisturbed current j_0 . The maximum value of j'_x , which is achieved at t_1 , is given over the volume of the cloud by

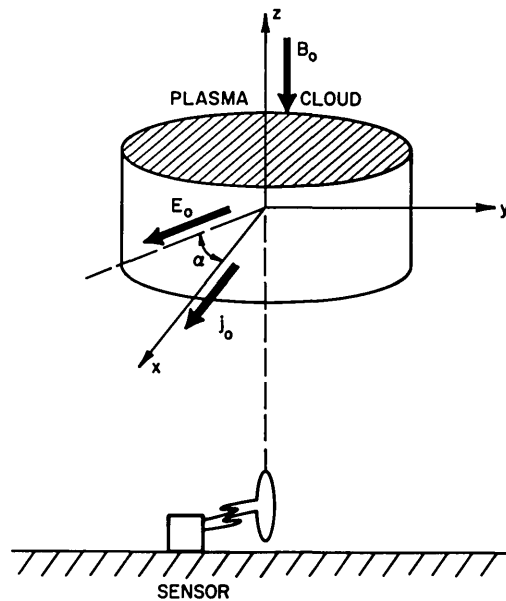


Fig. 5—Coordinate axes and background ionospheric-parameter relationships for plasma-cloud perturbation calculation

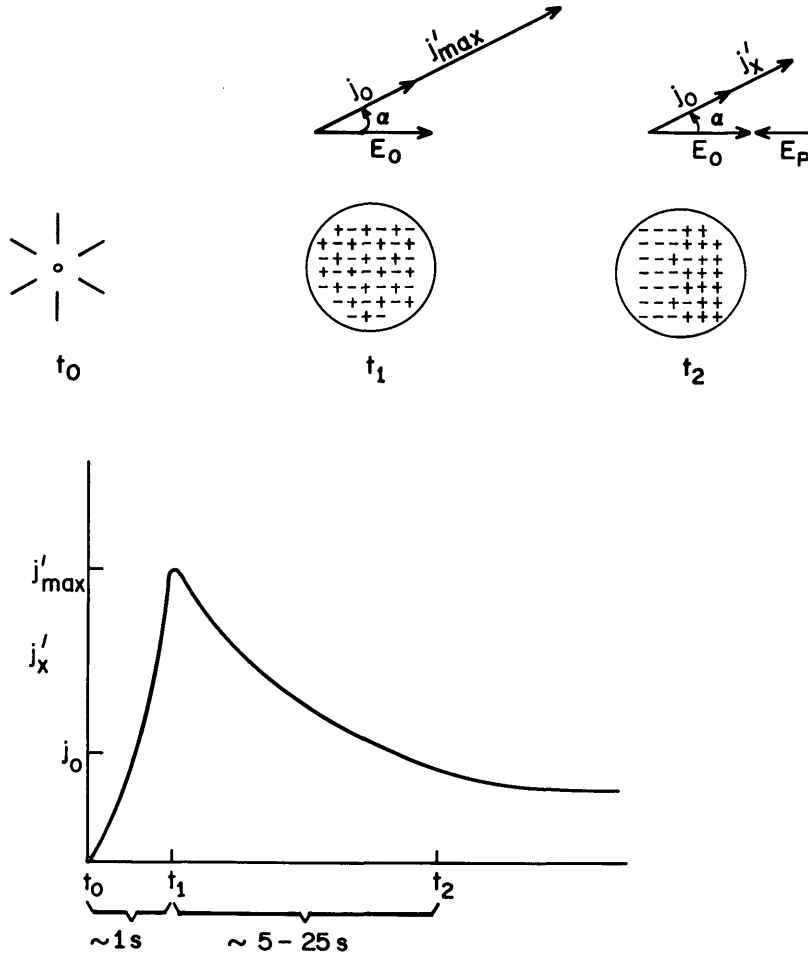


Fig. 6—Pictorial representation of the three stages of plasma-cloud evolution, with a sketched graph of perturbed current variation

$$j'_{max} = \frac{N' - N}{N} (\sigma_1^2 + \sigma_2^2)^{1/2} E_0.$$

We define a quasi-static perturbation magnetic vector potential $\mathbf{A}'(\mathbf{r}_1)$ at a point \mathbf{r}_1 outside the plasma column as

$$\mathbf{A}'(\mathbf{r}_1) = \frac{\mu_0}{4\pi} \int \frac{\mathbf{j}'(\mathbf{r})}{|\mathbf{r}_1 - \mathbf{r}|} dv.$$

Assuming N' , E_0 , σ_1 , and σ_2 to be constant over the volume of the plasma cloud, the perturbation magnetic field at a distant point $\mathbf{r}_1 = (0, y_1, -z_1)$ below the cloud is

$$(B'_x, B'_y, B'_z) \approx \frac{\mu_0}{4\pi} V_c \frac{j'_x}{r_1^3} (0, z_1, -y_1),$$

where V_c is the volume of the plasma cloud. For the point on the ground directly below the plasma cloud, assuming $\sigma_2 \gg \sigma_1$ in the lower E region,

$$B'_y(-z_1) \approx \frac{\mu_0}{4\pi} \frac{V_c}{z_1^2} \left(\frac{N' - N}{N} \right) \sigma_2 E_0$$

Assuming typical ionospheric parameters:

$$\begin{aligned} N' &= 10^3 N \text{ (for a cesium release)} \\ \sigma_2 &= 6 \times 10^{-4} \text{ mhos/m (daytime maximum value)} \\ V_c &= 10^{10} \text{ m}^3 \text{ (appropriate for a 50-kg payload at 100 km)} \\ E_0 &= 10^{-3} \text{ V/m} \\ z_1 &= 10^5 \text{ m} \end{aligned}$$

yields $B' \approx 10^{-11} \text{ Wb/m}^2 = 10^{-2} \gamma$. This quantity is at the lower limit of sensitivity for total-field measuring devices. Because the likely field instrumentation consists of induction sensors, a more appropriate quantity would be the time rate of change of the perturbation field, dB'/dt . Since hydrodynamic considerations indicate that the time scale of plasma-cloud expansion should be not greater than a few seconds, the quantity dB'/dt is likely to exceed several milligamma per second and is probably detectable with large loops of the kind used for the most sensitive geophysical observations. It is less likely, however, that remote sites would be able to detect an attenuated version of this perturbation, if indeed this perturbation is effective in stimulating a ducted wave. Though attenuation in the ionospheric waveguide is small, the portion of the disturbance field which is converted into such a wave is undoubtedly only a fraction of the total field magnitude. It is concluded that chemical releases in the temperate-zone lower ionosphere can permit, with present sensor technology, confirmation of the hypothesis that such means are capable of causing a significant disturbance in lower-ionosphere current flow. A modest effort is probably worthwhile simply to achieve this goal. The greater objective of measuring the ducted ULF waves which may be emitted by such a disturbance probably can be met only if the magnetospheric amplification process can be exploited (requiring chemical releases in the $L = 2.6$ to $L = 6$ band) or if magnetic sensor sensitivities can be improved by at least 20 dB (making it possible to determine whether conversion from the local perturbation to a ducted wave occurs with useful efficiency).

It should be noted that the achievement of sensor improvements is not simply a matter of lowering the sensor-system internal-noise power. The natural background noise from atmospheric and magnetospheric sources can often determine the sensitivity limit in the ULF band. This matter is discussed further in Part 4 of this report.

A second method of bringing about fluctuations in lower-ionosphere currents involves varying either the E-region electrical conductivity or the ambient dynamo currents by means of an indirect method, such as the collection of techniques known somewhat imprecisely as "ionospheric heating." There are several possibilities included in this general category, but prominent among them is the method of interaction with the ionosphere simply by radiating a large amount of RF power upward at a frequency equal to the plasma frequency of the region of altitude in which interaction is desired. Absorption of this power by the resonant electrons changes their kinetic energy and causes two consequences: (a) it alters their chemical reaction rates with the ambient ionic species, and (b) it results in expansion of the ambient plasma and concomitant reduction of density in the heated region. Calculations by Gurevich (31) indicate that in the lower ionosphere (heights less than 200 km) the decrease in the electron recombination coefficient dominates, which leads to a density increase; near the F-layer maximum (300 to 400 km) the key factor is the plasma expansion, which leads to a density decrease. In either case, it is evident that (except in the unlikely event that they counterbalance one another precisely) the electrical conductivity

of the region of the ionosphere illuminated by the RF heater can be altered. A possible method of changing the E-region conductivity then would employ a high-power RF heater capable of operation at typical lower-E-region plasma frequencies. In the normal daytime, a transmitter capable of operation in the 1.5- to 3.0-MHz band would serve this purpose. However, radio waves in this frequency range undergo as much as 20 to 30 dB of nondeviative absorption in the daytime D region, and it may not be possible with realizable transmitter power capabilities to heat the daytime E region by exciting it at its plasma frequency. At night, when the D region is absent and when the ducted waves which it is hoped would result from the excitation would experience the lowest attenuation, the necessary frequency band would be in the region of a few hundred kHz. Due to the weak currents and low conductivity which exist in the nighttime lower ionosphere, however, it is likely that substantially greater heating power would be required to yield a detectable effect in comparison to the daytime case. An alternative to plasma-resonance heating of the E region might be electron gyroresonance heating, in which the transmitter frequency would be matched to the frequency at which electrons gyrate about the magnetic-field direction. Such a method would have the advantage that the transmitter could be built to operate at a single frequency, which for mid-latitudes would be near 1.5 MHz and would be useful for both daytime and nighttime conditions. Its effectiveness would be higher in the daytime, of course, when a greater E-region electron density exists, but there would be no qualitative difference in its applicability under the two circumstances. It would also suffer the same daytime penalty of high D-region absorption as the plasma-resonance method.

An intriguing possibility which could have applications either in daytime or at night involves the phenomenon of sporadic E. Sporadic-E layers form in a largely unpredictable manner, but principally they form in the daytime at mid-latitudes and preferentially in the summer months. They are characterized by plasma frequencies of as much as 10 MHz (and even higher values on infrequent occasions), extend over areas of 10^{11} to 10^{12} m², and are located in the vicinity of 100-km altitude. It is likely that such layers, due to their high electrical conductivity, carry a large proportion of the local dynamo current and hence are attractive targets for artificial stimulation of ULF waves. For example, to achieve a perturbation magnetic field equal to that which was calculated previously for a chemical release of a plasma-cloud volume of 10^{10} m³, a typical intense sporadic E having a layer volume of 10^{15} m³ would require that its electron density be rapidly altered only by about 1%. A fractional electron-density change of 1% over a volume of 10^{15} m³ (equivalent to a 10-km thick sporadic-E layer of about 100-km lateral extent) might be achievable by RF heating. Heating an intense sporadic-E layer by the plasma-resonance technique would be possible at frequencies well above the range in which daytime D-region absorption is severe, and hence the main drawback of this method for E-region heating would be avoided.

This method of altering dynamo current flow might also be of interest in northern latitudes, where the phenomenon of "night E" is common (32). Often called high-latitude sporadic E, such layers of high charged-particle density in the nighttime E region might present an opportunity to combine the excitation of ULF perturbations in the lower ionosphere with access to the magnetospheric amplifier and to the low attenuation of ducted waves in the ionospheric waveguide. Moreover, the occurrence of night E is rather more prevalent (and predictable) than is mid-latitude sporadic E and would permit experiments to be conducted with less uncertainty regarding the probable adequacy of ionospheric conditions.

A promising method of E-region density modification has arisen recently with Showen's (33) demonstration that the lower ionosphere can be heated with transmitter frequencies above the local plasma frequency. Showen found that with a 40-MHz, 1-MW transmitter

operating (pulsed) for periods from 0.5 to 5 ms, electron-temperature increases of as much as 100% occurred in the D and E regions.

This type of heating occurs because the electrons are slow to dissipate energy acquired from the wave through collisions with the more massive neutral particles and ions. When this temperature rise is combined with the fact noted by Gurevich (31) and LeLevier (34) that the dissociative recombination coefficient of electrons with molecular ions is inversely dependent on temperature, it leads to charged-particle density growth. In the E region, for a typical daytime plasma frequency (2.8 MHz), this density change can occur on a time scale of as small as 10 s and grows asymptotically to one-half the percentage change in electron temperature (31). However, Showen's experiment did not produce detectable charged-particle density variations because of the very short transmitter pulses.

In addition to the high-power transmitter in Puerto Rico used in Showen's experiment, there is another ionospheric heater located at Boulder, Colorado, which operates in the 5 to 10-MHz band (35). Since the more northerly location is of interest for magnetospheric amplification, it is a useful exercise to see what changes are introduced in Showen's development by lowering the transmitter frequency to this range. At frequencies greater than the angular plasma frequency ω_p , the power dissipated per unit volume is given by Poynting's theorem as

$$Q = \frac{E_0^2 \Re \sigma}{2}$$

where σ is the conductivity of the medium and E_0 is the peak value of the oscillatory electric field. Ignoring ionospheric absorption, the wave electric field at height z is related to the transmitter power-aperture product PA_e by

$$E_0^2 = \frac{1}{2\pi^2} \left(\frac{\mu_0}{\epsilon_0} \right)^{1/2} \frac{\omega^2}{z^2 c^2} PA_e,$$

where ω is the angular wave frequency, c is the velocity of light, and μ_0 and ϵ_0 are the free-space magnetic permeability and electric permittivity respectively.

The ionospheric conductivity σ is very much dependent on the direction of propagation with respect to the magnetic field. If we invoke the quasi-longitudinal approximation for the vertically directed antenna (the magnetic dip angle at Boulder is 68°), then the conductivity may be written for each of the two characteristic wave polarizations, ordinary and extraordinary, as

$$\sigma_{o,x} = i\epsilon_0 \frac{\omega_p^2}{\omega \pm \omega_c \cos \theta + i\nu_e},$$

where θ is the supplement of the angle between the field line and the propagation vector, $\omega_c = eB_0/M_e$ is the electron cyclotron frequency, $\omega_p^2 = N_e e^2 / \epsilon_0 M_e$ is the angular plasma frequency squared, and ν_e is the effective electron collision frequency. From the Sen-Wyller correction to the collision frequency, we have $\nu_e = (5/2)\nu_M$ for $\omega > \nu_M$, where ν_M is the monoenergetic electron collision frequency.

Taking the real part of the conductivity and using the fact that $\nu_e \ll \omega \pm \omega_c$ for the regions of interest, we have

$$\Re (\sigma_{o,x}) \approx \left(\frac{5}{2} \right) \frac{N_e e^2 \nu_M}{M_e \omega^2} \left[\frac{\omega}{\omega \pm \omega_c \cos \theta} \right]^2.$$

At these lower transmitter frequencies it is necessary to account for losses in the wave amplitude which occur in the D layer. We can accomplish this by introducing an absorption term

$$E = E_0 \exp \left(- \int_0^z \kappa dz \right),$$

where $\kappa = \omega \mu_i / c$ and μ_i is the imaginary part of the refractive index. The refractive index is linked to the conductivity by

$$\mu^2 = 1 + \frac{i\sigma}{\epsilon_0 \omega}$$

from which

$$\kappa_{o,x} = \left(\frac{5}{2} \right) \frac{\omega_p^2}{2c\mu} \frac{\nu_M}{\left(\frac{5\nu_M}{2} \right)^2 + (\omega \pm \omega_c \cos \theta)^2}.$$

For most of the D region, $\nu \ll \omega$ and $\mu \approx 1$, so that if we define

$$-\ln \rho \equiv 2 \int_0^z \kappa dz,$$

then

$$-\ln \rho_{o,x} = \frac{2.65 \times 10^{-5}}{4\pi^2 (f \pm f_c \cos \theta)^2} \int_0^z N_e \nu_M dz.$$

Thus we obtain

$$\begin{aligned} Q_{o,x} &= \frac{1}{2} \left[\left(\frac{f}{f \pm f_c \cos \theta} \right)^2 \left(\frac{5}{2} \right) \frac{N_e e^2 \nu_M}{M_e \omega^2} \right] \left[\frac{1}{2\pi^2} \left(\frac{\mu_0}{\epsilon_0} \right)^{1/2} \frac{PA_e \omega^2}{z^2 c^2} \right] \left[\exp \left(-2 \int_0^z \kappa_{o,x} dz \right) \right] \\ &= \left(\Re \sigma_{o,x} \right) \cdot \left(E_0^2 \right) \cdot \left(\rho_{o,x} \right) \end{aligned}$$

Now we require that the electrons satisfy the energy-balance equation

$$\frac{dU}{dt} = Q(t) - (U - U_0) G_M \nu_M,$$

where t represents time, $U = (3/2)N_e k_B T$ = internal energy, T is electron temperature, and G_M is the fraction of electron energy lost per collision. Showen gives a value of 0.005 for this fraction. For $0 < t < (\text{transmitter pulse length})$ and letting $\tau_1 = 1/G\nu_M$,

$$\frac{dT}{dt} = \frac{1}{\tau_1} \Delta T_{ss} - \frac{(T - T_0)}{\tau_1},$$

with $\Delta T_{ss} \equiv 2Q\tau_1/3N_e k_B$ representing the steady-state change in temperature which would be achieved for the long-pulse-length limit. Making the simplifying assumption that τ_1 is constant, we can integrate the above equation. Let ΔT represent the change in temperature:

$$\Delta T = \Delta T_{ss}(1 - e^{-t/\tau_1}),$$

so that for $t \gg \tau_1$ it is clear that $\Delta T \rightarrow \Delta T_{ss}$. Evaluating ΔT_{ss} , we find

$$(\Delta T_{ss})_{o,x} = 72 \frac{PA_e}{z^2} \left[\left(\frac{f}{f \pm f_c \cos \theta} \right)^2 \rho_{o,x} \right],$$

where the quantity in brackets represents the additions to Showen's results due to the lower frequencies and the anisotropy of the medium. Thus ignoring for the moment the correction terms, with a power-aperture product of 10^4 MW m² at 100 km, a steady-state temperature change of 72°K is expected.

It is clear that without the D-layer absorption factor the temperature increase would be greatest for the extraordinary wave. However, when the integrated effects of absorption in the D layer is included, it is found that the ordinary wave is most efficient for E-layer heating. Accordingly, the calculations which follow refer to ordinary-wave propagation.

From LeLevier (34), in the lower ionosphere we can relate the percentage change in electron density to the percentage change in temperature by

$$\frac{\Delta N_e}{N_e} = \frac{1}{2} \frac{\Delta T_{ss}}{T} \left[\frac{\tau_2(1 - e^{-t/\tau_2}) - \tau_1(1 - e^{-t/\tau_1})}{\tau_2 - \tau_1} \right],$$

where, as mentioned above, $\tau_1 = 1/G_M\nu_M$ and $\tau_2 = 1/2N_e\alpha$, with α being the dissociative recombination coefficient. In the E region, $\tau_1 \ll \tau_2$, and we can write

$$\frac{\Delta N_e}{N_e} \approx \frac{1}{2} \frac{\Delta T_{ss}}{T} (1 - e^{-t/\tau_2}).$$

To evaluate the typical density disturbance resulting from a particular heating experiment, we adopt a daytime model ionosphere similar to that of Hanson, (36) and the COSPAR International Reference Atmosphere (CIRA) (37). The characteristics of these models are presented in Table 1 using a power-aperture product of 10^4 MW m² appropriate to the Boulder transmitter.

We have graphed in Fig. 7 ($t \gg \tau_1$) the asymptotic fractional change in temperature as a function of height for 5, 7.5, and 10 MHz and additionally for 40 MHz (to compare with Showen's case). In addition, we have given the time constant τ_2 for density growth as a function of height.

Table 1
Ionospheric Model Parameters

z (km)	N_e (cm^{-3})	T (°K)	ν_M (s^{-1})	α^* (cm^3/s)	τ_1 (ms)	τ_2 (s)
60	100	243.3	5.50×10^7	—	—	—
70	120	216.6	1.36×10^7	—	—	—
80	700	186	2.80×10^6	—	—	—
90	5.5×10^3	186	4.69×10^5	10^{-6}	0.43	91
100	10^5	213	8.30×10^4	6.3×10^{-7}	2.4	7.9
110	1.3×10^5	263	1.86×10^4	4.7×10^{-7}	11	8.2
120	1.4×10^5	381	5.48×10^3	3.6×10^{-7}	37	9.9

*Values for this quantity were obtained from A.P. Mitra and P. Banerjee, "Models for the effective recombination coefficients in the ionosphere," in *Space Research XI*, Vol. 2, K. Ya. Kondratyev, M. J. Rycroft, and C. Sagan, editors, Akademie-Verlag, Berlin, 1971, p. 1019.

Sizable variations in electron density are seen to be possible over time scales of tens of seconds. For example, at 100 km and 10 MHz the fractional change in electron density after one time constant $\tau_2 = 8$ s of continuous radiation would be (63%) $(1/2) (11.4\%) = 3.6\%$. It appears likely then that square-wave modulation of the HF heater with periods of approximately 5 to 10 s should cause periodic variation of the electron density over a large area. As with the previous methods of density perturbation, we expect this will modify the currents in the E layer and thus lead to a magnetic-field variation on the ground. To obtain some idea of the magnitude of this effect, we can proceed along the same lines as in the discussion of plasma-cloud releases. Once again a disk of increased density $N'_e = \lambda N_e$ is assumed to lie in the horizontal plane with a vertical background magnetic field. In this case, because of the longer time scales involved, we consider that the polarization fields have reached an equilibrium value. The geometry is the same as Fig. 5. The perturbed current in the equilibrium case is given by the usual electromagnetic boundary conditions and by conservation of particles (compare Martyn, Ref. 30). In the disturbed volume it is

$$j'_x = \frac{\sigma^2}{\sigma_1} E_0 f(\lambda),$$

where $\sigma^2 = \sigma_1^2 + \sigma_2^2$ and

$$f(\lambda) = \frac{\lambda - 1}{\left[(\lambda + 1)^2 + (\lambda - 1)^2 \frac{\sigma_2^2}{\sigma_1^2} \right]^{1/2}}.$$

This model has been used in other physical situations, notably by Chapman (38) in discussing eclipse-related ionospheric current disturbances. There are two useful limits of the preceding equations:

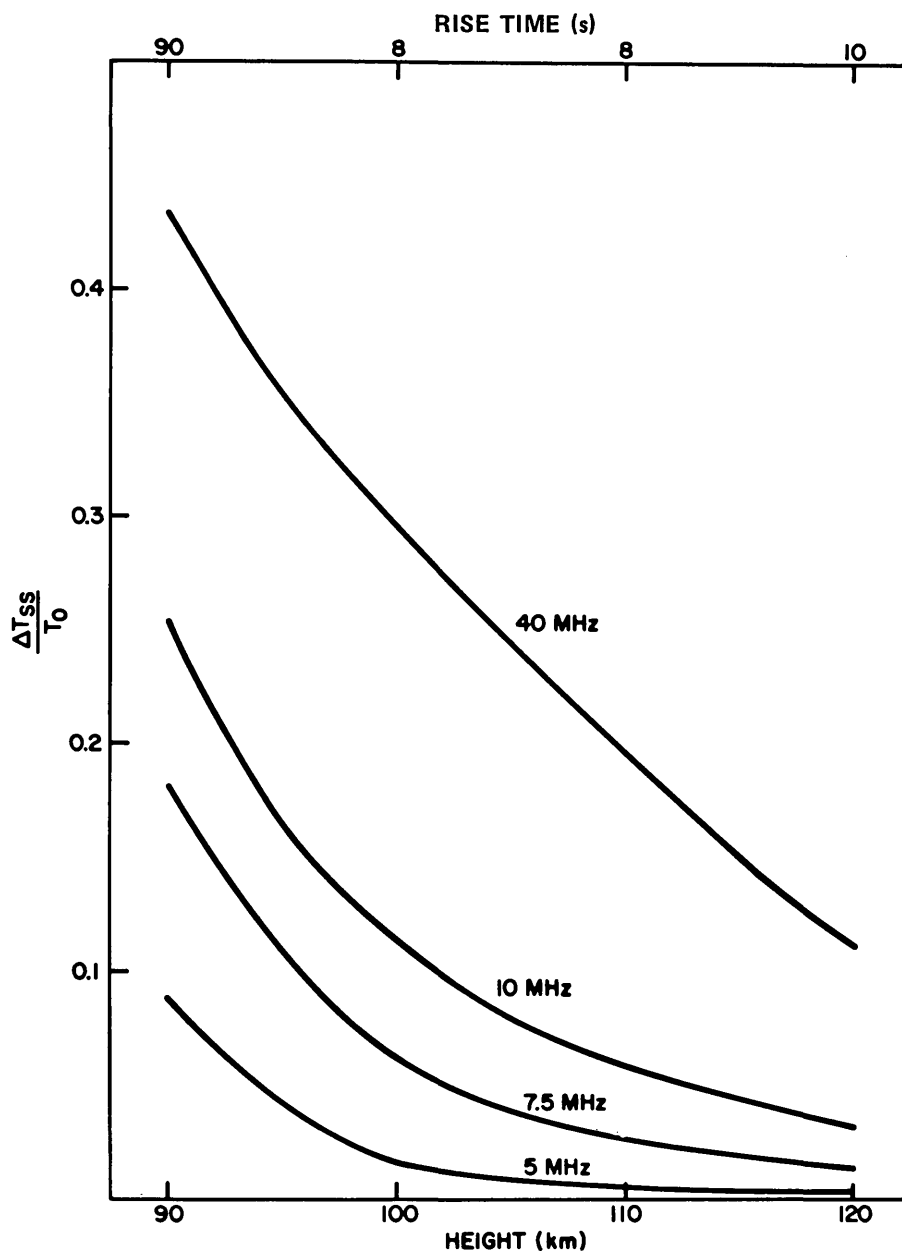


Fig. 7—Estimated steady-state effect (ΔT_{ss}) on E-region electron temperature (T_0) due to irradiation by Boulder ionospheric-heating transmitter with a power-aperture product 10^4 MW m². Characteristic time scales for electron density variations due to this process are indicated across the top for altitudes on the abscissa.

- (a) $(\lambda + 1)/(\lambda - 1) \gg \sigma_2/\sigma_1$, yielding $f(\lambda) \approx (\lambda - 1)/(\lambda + 1)$ and resulting in $j'_x \approx [(\lambda - 1)/(\lambda + 1)] (\sigma_2/\sigma_1) E_0$. In the E region $\sigma_2 \gg \sigma_1$. Thus

$$j'_x \approx \frac{(\lambda - 1)}{2} \frac{\sigma_2}{\sigma_1} \sigma_2 E_0 = \frac{(\lambda - 1)}{2} \frac{\sigma_2}{\sigma_1} j_0.$$

- (b) $(\lambda + 1)/(\lambda - 1) \ll \sigma_2/\sigma_1$, yielding $f(\lambda) \approx \sigma_1/\sigma_2$ and resulting in $j'_x \approx (\sigma^2/\sigma_2) E_0$. For the E region,

$$j'_x \approx \sigma_2 E_0 = j_0.$$

Approximation (a) is applicable to the particular case of a small perturbation extending over a large area. Typically σ_2/σ_1 might be about 25, so that if $(\lambda - 1)$ is equal to a few percent, the resulting perturbed current is about one-fourth the ambient dynamo current. If we again evaluate the near-zone field beneath the disturbance.

$$\Delta B \approx \frac{\mu_0 V_c j'_x}{4\pi z^2} \epsilon_y.$$

Assuming a background electrostatic field of 10^{-3} V/m, our model ionosphere yields $j_0 = 3 \times 10^{-7}$ A/m². The Boulder antenna has a 16° beamwidth at 7.5 MHz. Assuming a layer 10 km thick at 100 km gives a volume of 6×10^{12} m³. Substituting these values into the above equation, we obtain $\Delta B \approx 5$ m γ . Although this might be directly observable on contemporary instrumentation, coherent integration would be attractive for this method of ionospheric modification. In Table 2 the perturbed currents and magnetic fields are calculated under the same preceding approximations with a 3% density perturbation.

Table 2
Perturbed Current and Perturbed Magnetic Field at Four Altitudes

z (km)	j'_x (A/km ²)	ΔB (m γ)
90	0.002	0.10
100	0.130	7.70
110	0.080	3.90
120	0.020	0.87

The use of RF heating to cause changes in the dynamo currents may also be possible by an even more indirect method. It is believed that certain phenomena which take place in the F region may give rise to cross-field electromotive forces (electric potential differences between points displaced transverse to the geomagnetic field). A prominent example of such a phenomenon is spread F, which is an almost nightly occurrence at northern and equatorial latitudes and which occurs with somewhat less regularity at temperate latitudes (39 - 41). Because of the high electron mobility along the magnetic-field direction, such electromotive forces are transferred directly to the E region, where ion currents flowing horizontally close the loop. The Hall and Pedersen conductivities in the E region constitute the "load" in this equivalent electric circuit.

It has been found that RF heating of the F region produces effects which are quite similar to spread F (41), and it is reasonable to expect the F-layer irregularities which

result from the heating process to be transferred to the E region below. Electric potential differences which appear in the heated F region, such as might occur due to charge separation engendered in the plasma diffusion process, should also appear in the E region. These potential differences should alter the dynamo currents, which should accordingly cause changes in the local geomagnetic field. These changes represent possible candidates for ULF wave generation, provided they can be accomplished at a rapid enough rate.

It is not altogether clear at present that the F-region-heating method can result in E-region current fluctuations in the 0.5 to 5.0-Hz band. Most workers have found time scales of about 10 s to characterize the observed F-region response to RF heating (42,43). The results of Gurevich (31) described previously indicate that the transport processes which are operative at F-region heights are likely to constrain time scales for such phenomena to be of this order or greater. However, few, if any, careful attempts have been made to measure the E-region effects.

The RF heaters referred to earlier have been successful in stimulating the spread-F-like behavior which would be expected to have manifestations in the E region (42,43). Consequently, it would be worthwhile to place a ULF magnetic-sensor network in the vicinity of a suitable ionospheric heater for a simple experiment. Figure 8 shows such an experimental arrangement. The sensors are arranged, as in Fig. 4, on the orthogonal axes of a geomagnetic coordinate system, with a separation of a few hundred kilometers. One of them is located directly below that part of the E region that is connected by the geomagnetic field to the part of the F region which is illuminated by the ionospheric heater. The stippled region enclosed by the magnetic field lines which intercept the boundaries of the heated volume and the projection of that volume on the dynamo current layer below constitutes an equivalent electric circuit, which is shown in the inset at the upper left. Estimates of the size of the heated region lead to an effective loop area of 10^{10} m². Present evidence of the magnitude of this artificial spread-F effect is inadequate to estimate the size of the currents which flow in the dynamo-region (load) leg of the circuit.

An inherent advantage of the ionospheric-heating type of experiment over the chemical-release technique discussed previously is the greater control which can be exercised over experimental parameters. In the chemical release experiment, the ULF wave is essentially a transient, and sensors must correspondingly maintain a bandwidth adequate to pass the entire spectrum of the transient signal. This bandwidth may be several hertz. In the case of the ionospheric-heating experiment, the forced or driven response of the ionosphere is controllable by the modulation parameters of the heating transmitter, so long as the ionosphere will accommodate the appropriate wave spectrum. Although the transient or free response of the ionospheric medium will be superimposed on the desired signal spectrum, processing techniques can be used to discriminate in favor of the forced-response frequency. Allowable predetection signal bandwidths then are controlled only by the fluctuation spectrum of the ionospheric medium and can be made as narrow as this parameter will allow. Cross-correlation processing times of hundreds of seconds (bandwidths of hundredths of Hertz) may be possible, and a signal-to-noise-ratio advantage relative to the chemical-release case of several tens of decibels might be achievable. Such cross-correlation signal processing could be readily accomplished by simply comparing the band-limited ULF sensor output to a suitably demodulated replica of the transmitter waveform. This operation could be performed in the laboratory from data recorded on magnetic tape.

There remains to be discussed a hybrid version of the direct and indirect methods for altering the dynamo current. This method would employ an ionospheric chemical release whose purpose would be to change the ionospheric conductivity but which would

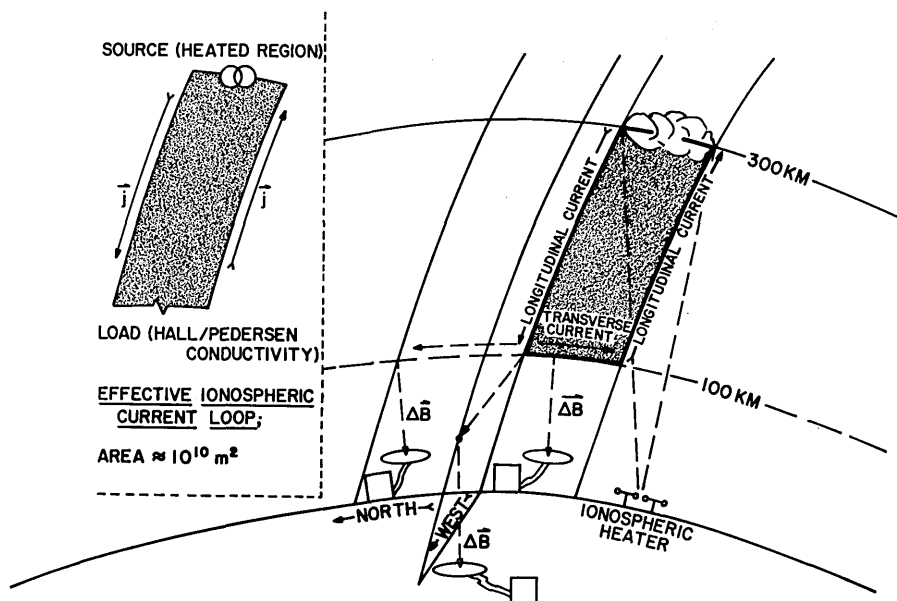


Fig. 8—Sensor network, heated region of the ionospheric F layer, and effective current loop in the ionosphere for one type of ionospheric heating experiment

require placement of the release in the F region rather than in the dynamo-current layer itself.

Present understanding of the movement of artificial plasma clouds in the lower F layer and the common appearance of internal striations is dependent on the principle described previously that shielding electric fields within a finite plasma cloud are neutralized by currents extending down to the E layer. A simplified picture of the physical process has been offered by Stoffregen (44) and is shown in Fig. 9a. The charge separation in the plasma cloud is dissipated by an electric current flowing to the E layer. This current is carried along the field lines between the F and E regions by electrons; in the E layer ions act as carriers because of their higher transverse mobility. A horizontal density gradient results; it is indicated at the bottom of Fig. 9a.

Stoffregen's experiment consisted of monitoring the 5577\AA emission (which is sensitive to electron and ion densities) in the area of the E region connected by magnetic field lines to the plasma cloud. Typical photometer records obtained in this manner indicate an apparent rise in emission amplitude at about 5 to 10 s after release, a time interval consistent with the ionization time of the plasma cloud (which was, in this case, barium). The analysis of these results yielded an estimated 5% variation in the E-layer electron density for the plasma cloud employed by Stoffregen over a region in the E layer comparable in size to the plasma cloud.

In a similar experiment involving a fixed-frequency sounding of the area of the E layer connected by magnetic field lines to the cloud, the data confirmed the occurrence of a local increase of this magnitude in the E-layer electron density.

Just as in the ionospheric-heating case described previously, the plasma cloud can be considered to be connected by nearly lossless conductors to the transverse-conductivity maximum in the E region below. Figure 9b is a schematic representation of the equivalent

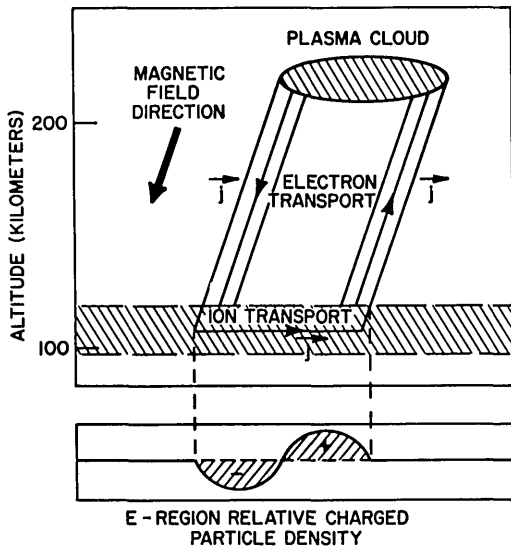


Fig. 9a—Charged-particle transport due to a plasma cloud in the F region

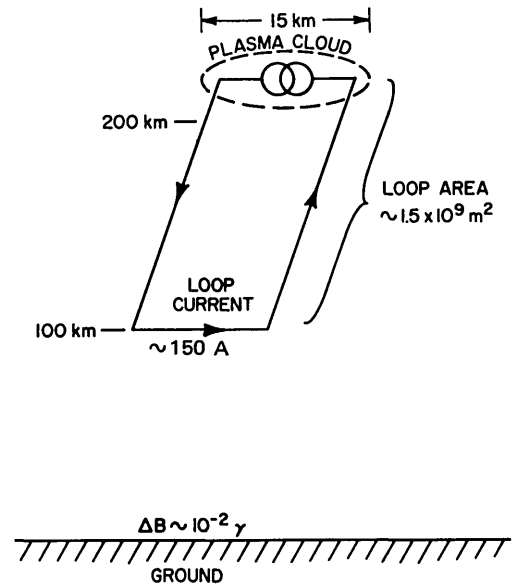


Fig. 9b—Ionospheric current loop due to the artificial plasma cloud deposited in the F region of ionosphere

electric-current loop in this case. If the interpretation of the optics experiment given by Stöffregen is correct, then an order-of-magnitude calculation ascribes to such a loop a current on the order of hundreds of amperes, estimated as follows. A number of electrons equal to 5% of the density of the E layer multiplied by one-half the volume of the plasma cloud moves from the cloud to the E layer in about a second. This transport time is probably the least known parameter, but based on the rapid onset of the E-layer effects observed, it is certainly no greater than 1 s. The magnetic field induced by such a loop is not large compared to the existing field, so that cloud motion is not significantly affected. The perturbation magnetic field induced on the ground in the plane of the ionospheric current loop is on the order of 10^{-2} gamma and is polarized perpendicular to the plane of the loop. Assuming that the change which takes place in the magnetic field measured on the earth occurs in less than 1 s, an induction device capable of detecting $10^{-3} \gamma/\text{s}$ variations should be adequate. Achievement of an adequate signal-to-noise ratio will require that a method of discriminating against background micropulsation noise be devised; a long-baseline gradiometer technique with orthogonally placed sensors similar to those illustrated in Figs. 4 and 8 should suffice.

Stimulation of Wave-Particle and Wave-Wave Interactions in the Magnetosphere

There are two types of interactions involving stimulated emission of ULF waves in the magnetosphere which could be investigated. The methods employed to achieve this stimulation bear a superficial resemblance to the two general types of stimulus described above—one of them involves injection of charged particles and the other involves use of a high-power radio transmitter. In both cases, however, the principle involved is quite different from those described previously. Whereas in the prior examples the techniques involved essentially the creation of a radiating system by modulating current passing through an essentially linear equivalent circuit, in the present cases both methods involve the exploitation of a nonlinear property of the trapped-proton belt. In contrast to these prior

examples, no quantitative estimate can be made of the likely achievable wave magnitudes. The discussion accordingly will be limited to a qualitative one.

Based on the presumption that Pc 1 micropulsations result from the spontaneous response of a latently unstable energy/pitch-angle distribution of protons in the near-equatorial $L = 2.6$ to $L = 6$ magnetospheric region, it might be possible to inject, artificially, charged particles into the magnetosphere in sufficient quantity to achieve this state of instability. The likelihood that such an endeavor would succeed in distorting the overall energy/pitch-angle spectrum (that of the resident particles plus the added ones) has been discussed by others in some detail but must be regarded as rather uncertain.

Estimates based on present knowledge of the resident-proton population indicate that several kilograms of ions injected into the $L = 3$ to $L = 4$ magnetospheric region might suffice to create the desired condition of instability (22). For this operation to cause amplification of waves in the 0.5- to 5-Hz band, the ionic species must be a light one, and lithium would be an attractive choice. The material could be ejected from a rocket or satellite launched into the precise desired position, which would require a high trajectory and consequently a large and rather sophisticated vehicle. Alternatively, it could be injected at relatively low altitude (just above the collision-dominated region of the atmosphere, so that the injected material would not be impeded by local particles) by a shaped-charge or ion-beam generator oriented along the direction of the geomagnetic field. The latter method has appeal because the charged beam would be collimated by the magnetic field and hence could be confined to the desired magnetic field lines. It is not known whether lithium or other light-ion beam generators could be constructed to deliver a large enough number of ions, and the ion-beam method is likely to be expensive. A shaped-charge injection method would permit *neutral* lithium to be emitted in a desired direction and would rely on photoionization to ionize the particles as they proceed to the equatorial plane. The ionization time of lithium, which is several tens of minutes, could allow the particles to proceed toward the desired region of the magnetosphere during the ionization process. The beam would be less well collimated than that which would be emitted from an ion-beam generator, of course, but several uncertainties would be avoided. The photochemistry and thermodynamics of the lithium-ion cloud would be predictable and well understood, and the conditions established after formation of the ion cloud in the magnetosphere would be known. Performance of a large ion-beam generator would not be well known, due to possible neutralization difficulties, and the interactions of the intense ion beam with the magnetic field and exospheric plasma would be unpredictable. For example, the beam might striate, achieving a highly irregular structure by the time it arrives in the equatorial region.

Measurement of the effects of this plasma-injection operation on ULF waves would involve a slightly more complicated arrangement than has been described in the preceding. Instrumentation should be located at *both* terrestrial terminals of the geomagnetic field lines along which the plasma is injected, and orthogonally displaced sensor networks should be established in at least one of these terminal regions. Baselines should be much longer than in the previous examples, because of the larger probable geographical extent of the effects, and a larger number of stations should be used. In the western hemisphere, the likely locations are either the New Zealand-Alaska conjugate pair (about $L = 2.8$) or the Antarctica-Canada conjugate pair ($L > 4$). The former seems to be more convenient logistically.

Fortunately the frequencies of interest for ULF waves associated with ionic lithium in the $L = 2.8$ region are centered on 1.5 Hz, corresponding closely to the frequency band

occupied by Pc 1 micropulsations. Sustained interest for several decades has yielded considerable experience in dealing with the noise background and in devising apparatus for detecting signals in this band. The initial experiment should probably be conducted under darkened conditions at both terminals to reduce the number of experimental variables, and so a near-equinox period would be appropriate. Observations should show an increase in micropulsation activity coincident with the entrance of the plasma cloud into the equatorial magnetosphere. Once again, as in the case of the chemical releases described previously, the desired signal will be a transient-like manifestation of the free response of the system (although in this case it may be an extended sequence of pulses due to the regenerative properties of the magnetospheric amplifier and its transmission lines terminated in the ionosphere). Sensors should be arrayed so that this signal may be distinguished from background micropulsation noise.

Under certain circumstances, it may be possible for energy to be coupled not only between gyrating particles and MHD waves but between waves of different types in the magnetosphere (23,24). For example, a three-wave interaction could involve two VLF waves (which might be considered analogous to the "pump" and "idler" waves in a laser or parametric amplifier) interacting to yield a wave at the difference frequency (the "signal"), which might fall in the ULF band. Such an interaction would require very high pump-wave field strengths in the interaction region, and it is precisely for this reason that VLF pump and idler waves are proposed.

The virtue of employing a VLF pump and idler, provided the antenna requirements can be met, is that the magnetospheric trapped-*electron* belt causes amplification of VLF waves in a manner directly analogous to that described previously in which trapped *protons* (or ions) can amplify ULF waves. Indeed, the amplification limits for VLF waves may exceed by far the limit of 30 dB or so indicated for ULF waves. VLF waves in the magnetosphere are also channeled to a certain extent along the direction of the magnetic field by virtue of their characteristic wave properties, although this channeling is far less efficient than in the analogous ULF case (45). However, a process of ducting along the magnetic field by field-aligned filaments of charged-particle density enhancement has been found both theoretically and experimentally to act as a most efficient means for directing VLF power along the magnetic field between the lower ionosphere and the trapped-particle belt (45).

Consequently, it may be possible to transmit VLF pump and idler waves of the proper polarization from below the ionosphere into field-aligned ducts which will direct them into the region of the magnetosphere where they can be amplified by electron cyclotron interactions with trapped electrons. The amplified VLF waves may then exceed the threshold for commencement of a three-wave process whose product will be the desired ULF signal. This signal, which may undergo further amplification due to cyclotron interaction with the resident protons, can then descend to the earth through a series of interactions analogous to those which are appropriate to Pc 1 micropulsations and be detected by earth-based sensors. Because the VLF transmitter is controlled, coherent integration may be used for signal processing, with a predetection bandwidth narrowed about the modulation spectral peak (the difference frequency between pump and idler) to as narrow a passband as the propagation medium and operational considerations will allow. Bandwidths of hundredths of hertz would seem to be allowed because VLF magnetospheric ducts normally have lifetimes of tens of minutes.

To properly assess the possibility that a three-wave process involving VLF pump and idler waves and a ULF signal wave can take place in the magnetosphere, it is necessary to consider the three-wave interaction problem in a plasma in which both electrons and ions

are active participants. To our knowledge, the only analysis of three-wave processes at VLF has ignored ion motions (23,24). For a simple case of strictly longitudinal propagation of all three waves, a case which could be treated easily, it is not possible to satisfy the conditions of synchronism (summation of signal and idler frequencies to equal the pump frequency and similar vectorial summation of the respective wave vectors) except for signal and pump frequencies very near the electron cyclotron frequency. Such frequencies are outside the range of natural VLF amplification. However, because VLF whistlers can have wave vector directions of approximately 10° to 20° away from the magnetic-field direction, there remains the possibility that oblique whistler waves can satisfy the synchronism requirements. There is evidence, albeit slim, that three-wave interactions may occur naturally. As we mentioned above in Part 2 of this report, Fraser-Smith (25) has suggested that atmospheric discharges may be a cause for Pc 1 micropulsations, and if so, a three-wave interaction could be the coupling mechanism.

It is of interest to examine the means by which a VLF-ULF three-wave interaction experiment might be conducted. To bring about magnetospheric amplification of VLF pump and idler waves, so that the relatively weak fields of earth-bound transmitters may be increased to the magnitude which is necessary to trigger the interaction, it is necessary to consider the typical frequency ranges in which such amplification is observed naturally and to investigate the sites of available VLF transmitters. According to Liemohn (11), VLF whistlers are most commonly observed at between $3/10$ and $5/10$ of the equatorial electron gyrofrequency (ω_{ce}) on the magnetic field line which passes through the ionospheric entry point of the whistler. For Pc 1 micropulsations the frequency range is between $3/10$ and $7/10$ of the equatorial proton gyrofrequency (ω_{ci}) along a similarly defined magnetic field line. Assuming an earth-centered dipole as a crude approximation to the magnetic field of the earth, these gyrofrequencies are related to geomagnetic latitude λ on the earth by

$$\omega_{ce} = 5.5 \times 10^3 \cos^6 \lambda$$

$$\omega_{ci} = 3.0 \times 10^6 \cos^6 \lambda$$

Figure 10 illustrates the frequency bands in which VLF and ULF amplification might be possible under these conditions vs geomagnetic latitude, with ULF frequencies on the right-hand scale. The latitudes, available tuning ranges, and normal transmitting frequencies of three U.S. Navy VLF stations (NPG, NAA, and NSS) are shown superimposed on the curves. Although the tuning ranges available to NPG and NSS include a substantial part of the amplification band, only NSS has a normal operating frequency within this band. Also, NPG and NSS are at such low latitudes that the favored ULF frequencies are above about 7 Hz. Furthermore, NSS is below the nominal $L = 2.6$ lower extreme of the region in which magnetospheric amplification of ULF waves is believed possible. For NAA, noting that the lower extreme of its tuning range approaches the VLF amplification band for that latitude, it may be possible to create ULF waves at a frequency below 5 Hz.

This combination of circumstances would favor station NAA as a candidate for an experiment. An additional factor which may influence the preferred ULF frequencies involves the likelihood that launching VLF waves into the magnetospheric duct appears to be favored for waves entering the ionosphere from the north (45). Consequently the actual field line along which the VLF pump and idler waves are launched may be a few degrees lower in latitude than the transmitter location, and the preferred ULF frequencies will thus be somewhat higher.

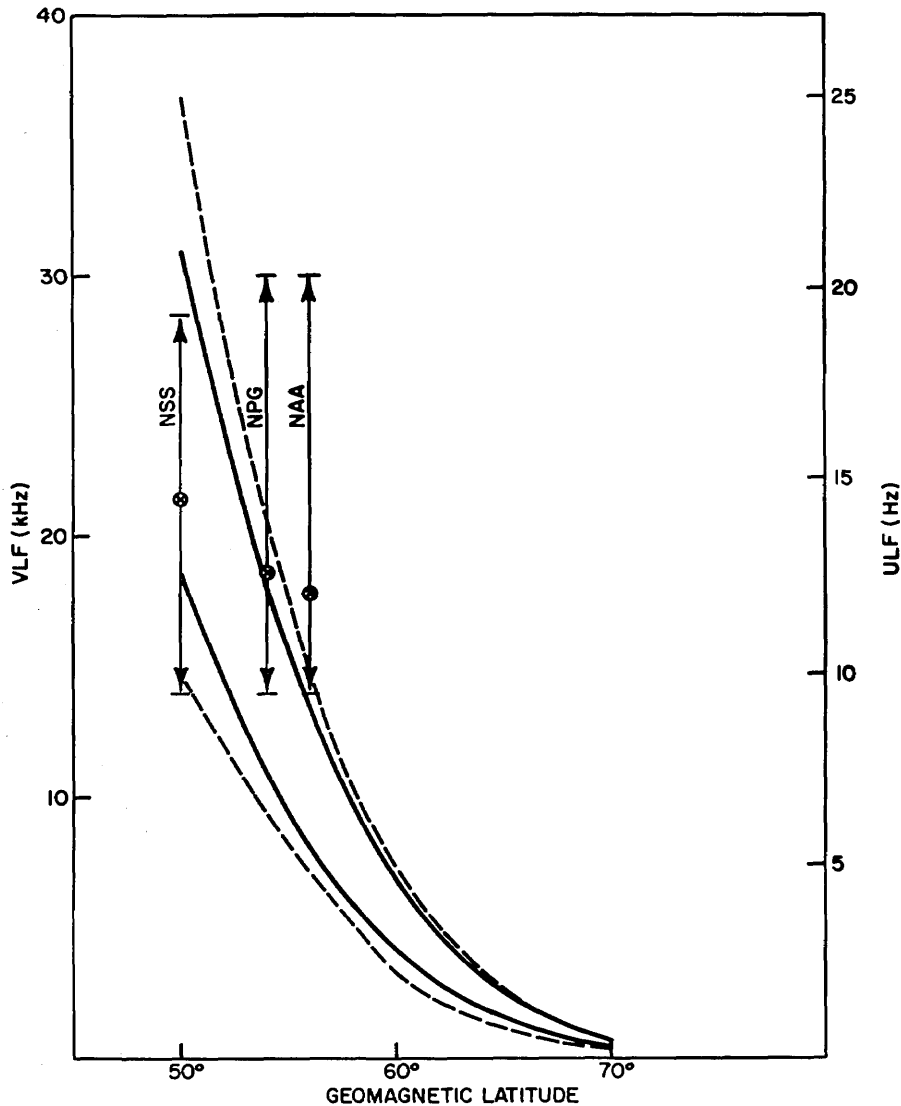


Fig. 10—VLF transmitter frequencies (solid lines) and ULF modulation bands (dotted lines) appropriate to the magnetospheric three-wave interaction experiment for three U.S. Navy VLF transmitters

4. EXPERIMENTS PROPOSED AND IN PROGRESS

Apparatus

ULF waves in the 0.5 to 5-Hz band can be detected by induction devices and by capacitive devices, both of which require a special design. The field strengths associated with geomagnetic variations at these frequencies are quite small, and the dynamic range of the various signal and noise components which must be accommodated is very wide. The types of instrument which are required for this function tend to be physically large to provide adequate collecting aperture; hence they can be affected by sonic and seismic stimuli and by air motions and precipitation. All of these factors must be taken into consideration not only in the design of the apparatus but in placing it in field locations and in

instrumenting for data recording and signal processing. For example, in an area in which thunderstorms are common, it would be unwise to rely on a sensor which is sensitive to air motion, precipitation static, and environmental conductivity changes. A monopole antenna for detection of the vertical electric-field component thus would be impractical. In an area where, in addition to these complications, the soil is not suitable for excavation, it would not be prudent to attempt to use large air-core induction sensors having a radius of several feet, because they could not be buried to escape thunder- and wind-related vibration noise. Under such circumstances, ferromagnetic-core inductors would be more practical. Electronic instrumentation would have to have a linear dynamic range of several orders of magnitude to prevent atmospheric discharges from severely contaminating the data whenever thunderstorms occurred within a few hundred miles.

There are two basic types of induction sensors. A class of inductors designed by Campbell and his associates at the National Oceanic and Atmospheric Agency consist of air-core loops with a diameter of 2 m, wound with several thousand turns of 0.127-mm copper wire. An investigation of several antenna types culminated in a 16,000-turn design, which provided the best combination of ease of winding, sensitivity, and antenna mobility (46).

We have found these inductors to be rugged and easily handled by two or three men. They may be trucked to remote locations readily. They have several disadvantages, however. They are physically large and must be rigidly mounted to an immovable support to avoid motion-related noise signals due to wind and sound stimuli. In practical terms, this means they must be buried in a trench 7 ft deep. There are many locations in which it is impractical to excavate to such depths. Indeed, many desirable field sites are located in mountainous areas where man-made electromagnetic noises (rotating machinery, high-voltage switching transients and surges, and power-main leakage fields) are low enough to permit the inherent sensitivity of the antennas to be realized. Other examples in which excavation is not possible include swampy areas, where water tables are only a few feet or inches below the surface, or areas so remote that mechanical ditching equipment is unavailable. This drawback is considered to be a serious one for any application in which the convenience of placement of the inductors is a dominant consideration.

There are two other disadvantages. First, in a buried configuration the inductor must be wedged into a ditch, which cannot actually be backfilled if the inductor is to be retrieved. In such a configuration, ground water or soil particles dropping into the ditch create a noise signal which can be significant. Second, the 60-mi length of wire which is used in each antenna results in an antenna output impedance (predominantly resistive) of about 130 k Ω . Thus, whereas the antenna *itself* has a noise level of tenths of microvolts (and hence is inherently sensitive to geomagnetic signals as small as a few tenths of a milligamma at 1 Hz), it is difficult to realize this sensitivity. Amplifiers which will match this impedance level in the 0.5 to 5-Hz frequency band are typically noisier than the loops.

For our application we have attempted to band-limit noise of all types by placing a set of low- and high-pass filters on the preamplifier output terminals. Typical passbands are shown in Fig. 11 and are arranged to discriminate in favor of ULF waves in the vicinity of 0.5, 1.25, and 3.0 Hz respectively. Discrimination against power-line frequencies is achieved by a notch filter. Further discrimination against the higher frequency components of local atmospherics is achieved by insertion of a small amount of ac-coupled negative feedback around the preamplifier. Further means, which may be useful to reduce the effects of noise from remote atmospheric discharges, are described later under ULF Noise Investigations.

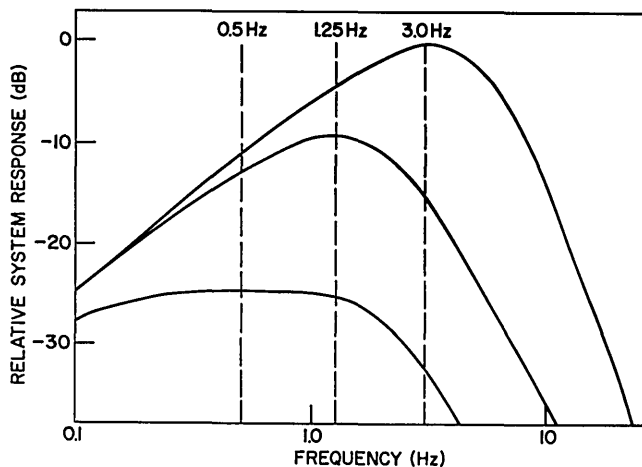


Fig. 11—Response curves for air-core induction antennas and associated electronics

It is essential to prevent large transients, which usually are due to lightning strokes whose low-frequency components are propagated in the earth-ionosphere waveguide, from driving the preamplifiers into a nonlinear operating regime. We have thus maintained a linear dynamic range of about 80 dB in the preamplifier system (exclusive of negative feedback at the high-frequency extreme). For this purpose we also have maintained 60 dB in a data-recording system now under procurement (in the past we have used an analog tape recorder whose linear dynamic range is about 40 dB).

Practical ferromagnetic-core inductors are capable of the same degree of sensitivity as the large air-core loops and have some important advantages over them. They are somewhat more portable and, for example, can be transported aboard most multi-engine aircraft. This advantage is quite a valuable one for field operations in remote areas where it is seldom convenient, and often impossible, to arrange transportation via an aircraft with a 7-ft cargo door. Also, these sensors are physically smaller and are less subject to sonic and wind stimuli. They may be simply placed on the ground and sandbagged for stability. Finally, the ferromagnetic-core devices require only a small fraction of the wire length which the air-core devices require to achieve the same sensitivity. This wire can, in addition, be of a larger diameter. Both of these circumstances lead to a much lower antenna resistance. A typical resistance level is a few hundred ohms, and preamplifiers can be constructed in this range of input resistance which will permit the tenths-of-microvolts antenna noise limit to be realized.

The principal potential drawback of the ferromagnetic-core inductors is their inherent nonlinearity. These devices operate on a hysteresis curve, and the nonlinearity of this curve can cause odd-numbered harmonics of a large signal or intermodulation products between a large signal and smaller ones to degrade its performance. Less important, but possibly significant, are Barkhausen noise, magnetostriction effects, and changes in the magnetic properties of the core material, all of which may degrade the performance of the inductor (46).

At this writing, it is not possible to state whether these possible limitations of ferromagnetic-core inductors are important for the measurement of low-intensity waves in the ULF band. It is not likely that intermodulation components of atmospheric combining

with signals in the frequency range of interest will often be of concern. The dominant spectral components of all except local atmospherics fall in the band above about 8 Hz and hence would pose a problem only when ULF frequencies above about 4 Hz are of interest. Local atmospherics will probably cause either type of induction sensor system to react nonlinearly, simply by overdriving the preamplifiers.

A thorough investigation is planned of the potential drawbacks of ferromagnetic-core inductors, based on comparison of their performance with that of air-core sensors. At present there is on hand a set of 8000-turn mu-metal loops, approximately equivalent in sensitivity to the air-core devices described previously. Figure 12 contains several system response curves for the mu-metal sensors and their associated electronics. The response curves are shaped somewhat differently from those in Fig. 11, partially because more sophisticated high-pass filters permitted the skirts of the passband to be sharper (thus permitting the center frequencies to be raised somewhat, with the same rejection of high-frequency components). In the center curve of Fig. 11 and the right-hand curve of Fig. 12, for example, the high-frequency -30-dB point falls just above 11 Hz. If these two curves are laid over one another so that their peaks are at the same level, it will be found that they match reasonably well, with crossing points at 0.7, 1.6, and 11.0 Hz.

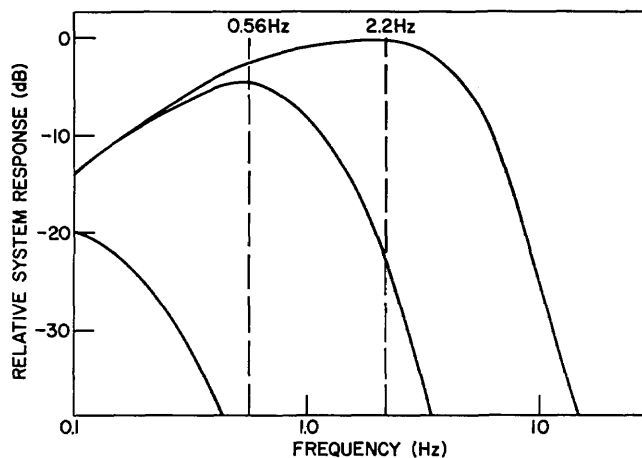


Fig. 12—Response curves for mu-metal-core induction antennas and associated electronics

Electric-field sensors are of two types. Earth-current probes provide a means of measuring the electric potential between two points near the surface of the earth and hence make it possible to determine the horizontal-plane electric-field components. These field components are the electric equivalent to a portion of the magnetic fields to which a three-loop system is sensitive. For an electromagnetic wave normally incident on the surface of the earth, for example, two horizontal, orthogonally oriented earth-probe pairs would receive the same signal as would two suitably oriented horizontal-axis inductors. For waves incident from an off-normal direction, such as atmospherics propagated via the earth-ionosphere waveguide, no such simple correspondence exists. This feature is of some value for direction-finding and discrimination against waves traveling by one mode in favor of those traveling by another and will be discussed in greater detail later under ULF Noise Investigations.

Earth-current probes have one main attraction—they can readily be made 10 to 20 dB more sensitive than practical induction antennas. For investigations in the 0.5 to 5-Hz region, however, they have little overall advantage because they are quite sensitive to environmental effects associated with precipitation and temperature changes. Moreover, it is difficult to perform cross-correlation signal processing with pairs of sensors in different locations, due to biasing problems associated with contact potential differences between the probes and the soil and to difficulties in calibration.

The second type of electric-field sensor is one which is capable of measuring the vertical electric-field component. Examples of such a sensor include primarily capacitive devices such as simple monopole antennas and their refinements as embodied in ball (47) and parallel-plate antennas. All of these devices essentially measure the vertical electric-field component between an elevated, insulated conductor and the ground or between two such conductors with as great a degree of isolation from the ground as possible. Because this isolation can never be perfect, these sensors are subject to vibration, to changes in ground conductivity, and to motions of nearby (grounded) objects. Provided that adequate provision can be made for isolation of vertical electric-field sensors from these sources of noise and for calibration, they are of value because they permit certain information to be gained which cannot be easily acquired from a three-loop system. This matter also will be discussed in the following section.

The phenomena we have described above and the ULF noise we discuss in the following section typically can be expected to range in amplitude from below the sensitivity limit of less than 1 m γ at 1 Hz, which the induction sensor systems permit, to a level several tens of decibels higher. Under conditions of geomagnetic quiescence and in the absence of strong atmospheric interference, the background noise can be less than this sensitivity threshold. Consequently, it is desirable to consider other sensing techniques which could permit greater sensitivity.

Laboratory magnetometers employing the quantum mechanical Josephson Effect in superconductors have been shown to have a sensitivity better than 0.01 m γ . Because these devices operate at liquid-helium temperatures, however, they have not been considered until recently as practical sensors for geophysical investigations. Advances in Dewar-container technology now would seem to permit the use of this type of cryogenic magnetometer in the field for periods of about two weeks without replenishing the coolant, and it thus is feasible to use them for investigations of the type we have discussed. It is likely, however, that substantial engineering effort will be required to adapt this laboratory instrument to the physically punishing conditions of geophysical field operations.

ULF Noise Investigations

From the standpoint of signal-to-noise ratio, the noise environment in which a low-level signal must be discerned is equally as important to a communicator as the signal itself, because he can exploit whatever statistical or morphological characteristics the noise possesses to enhance his probability of extracting signal material from it. This fact is of particular importance in the ULF band, because noise in this frequency range is characterized by a number of strong qualities which may readily be exploited.

Prominent among these characteristics is polarization. Lightning discharges (atmospherics) are often the major source of the low-level background at frequencies above about

1 Hz. In the absence of nearby atmospheric activity, the average background level is about 1 m γ /Hz, a level we have surmised from the limited data available (47). To our knowledge, no thorough study has been conducted of nongeomagnetic noise below the Schumann resonance band. (It is part of our planned effort to conduct such a program.) As an indication of the severity of this noise level, it should be noted that geomagnetic micropulsation activity is practically undetectable above about 3 Hz in the presence of noise (48). This background noise arrives at a temperate-latitude site by propagation in the earth-ionosphere waveguide from the usual sources of distant atmospheric discharges, which are predominantly in the equatorial zone. The propagation mode by which this noise travels in the earth-ionosphere waveguide is analogous to the TEM waveguide mode. It is characterized by electric and magnetic field constituents which are both transverse to the direction of propagation, with an electric field which is wholly vertical and a magnetic field which is wholly horizontal. The fields of this noise are nearly uniform over the altitude interval from the surface of the earth to about 80 km.

Geomagnetic noise in this frequency range is somewhat more complex. Directly beneath the source region in the lower ionosphere, the signal which is received on the ground is a quasi-evanescent component of the fields generated in the ionosphere by the slow Alfvén wave which is incident from the magnetosphere. These fields are a superposition of the left-hand-circularly-polarized primary wave and a local right-hand circularly-polarized fast or isotropic Alfvén wave which is generated in the lower ionosphere (nominally at a 100-km altitude) by the incoming wave (21). Thus the polarization below the source region is generally elliptical and can be of either rotational sense, depending on the time of day. (Attenuation of the left-hand-polarized incident wave is always high in the lower ionosphere, but the wave is guided preferentially downward, and hence its power is concentrated in that direction. Attenuation of the right-hand-polarized secondary wave is much higher in daytime than at night, and in addition its power is distributed isotropically (1,18,49).) However, the *electric*-field resultant of this pair of superimposed waves is nearly horizontal and has a vertical component only to the extent that the magnetic field lines in the direction of wave incidence depart from the vertical. In the $L = 2.6$ to $L = 6$ region the geomagnetic dip angles are typically 70° or larger, and so this vertical electric component is quite small.

ULF waves travel away from the source region by a ducted, isotropic Alfvén mode in a waveguide which extends between about 100 km and about 2000 km above the earth. It is characterized by a purely horizontal electric field and by a magnetic field whose horizontal projection is very nearly in the direction of propagation (2,50). This orientation is precisely in the propagation direction only for the case in which the background magnetic field is purely vertical or for geomagnetic east-west propagation. It is close to the direction of propagation at high and middle geomagnetic latitude for any background field direction. As a consequence of the difference in propagation characteristics, a micropulsation and an atmospheric discharge originating at the same point and traveling, each by its appropriate mode, to a temperate-latitude receiver would have nearly orthogonal electric and magnetic fields. It is evident then that judiciously oriented induction sensors could permit one class of signal (or noise) to be selected over the other.

Furthermore, a suitable combination of the outputs from electric and magnetic sensors could readily be used to subtract the contribution of one class of signal in *any* source direction from the total received power. Suppose, for example, that a particular source region for ducted Alfvén waves is to be favored. Suppose further that atmospheric sources in other directions are contributing to the noise which contaminates this signal. An induction sensor can be oriented with its axis horizontal and in the direction of the desired

Alfvén wave source. Atmospheric noise will be received by this sensor in the degree to which its axis is transverse to the noise source directions. This noise could be partially removed by subtracting from the induction-sensor output the output of a vertical-electric-field sensor, which would be sensitive only to the atmospheric wave. A similar technique would be useful in discriminating among source directions for ducted Alfvén waves and could, for example, be used to remove a part of the geomagnetic micropulsation noise from a ULF signal traveling in a different direction.

A second technique is available for improving the signal-to-noise ratio of a selected ULF signal. Atmospherics traveling in the earth-ionosphere waveguide have a group velocity which approaches the speed of light. Ducted Alfvén waves, on the other hand, travel at several hundred kilometers per second (6,7). Consequently, by separating identically oriented sensors of the same type by a distance of a few hundred kilometers, the ULF component of distant atmospherics from all directions can be attenuated relative to the ducted Alfvén waves simply by subtracting the outputs of the two sensors. Similarly, ducted Alfvén waves from one source direction can be selected relative to those from another direction by translating the two sensor outputs in time relative to each other by an amount equal to the propagation time of the undesired waves between the receiving locations and by then subtracting them.

Three circumstances combat the effectiveness of these methods, and it is, indeed, the purpose of our ULF noise program to determine their degree of effectiveness. First, the magnetic field of a ducted Alfvén wave associated with a micropulsation signal is seldom purely linearly polarized. It is, more commonly, elliptically polarized with a right-hand sense and with the major axis of the polarization ellipse oriented along the propagation direction (2,21). It is often observed that narrow-band Pc 1 micropulsations have a polarization ellipse with higher eccentricity than broadband Pc 1 or Pi 1 micropulsations; thus it is likely that the ellipticity is a result of the phase relationships between frequency components. It can be reduced possibly by narrow-band filtering, especially if cross-correlation signal processing is used for artificially generated ULF signals.

Second, large-scale irregularities in the electrical conductivity of the earth can distort the wave-field orientations and cause polarization irregularities to appear (51). For example, ducted micropulsations should have no vertical magnetic-field component. Yet in the vicinity of massive geological anomalies and seashores with rapid dropoff, a substantial vertical component is detected (52). In the neighborhood of pronounced earth-conductivity discontinuities that occur at the shores of midocean islands, such as Bermuda, the vertical component can equal the horizontal component in magnitude (53). However, beyond a few kilometers from, for example, the western coast of Canada (52), such seashore effects appear to be negligible. Despite the fact that large conductivity discontinuities can affect the use of signal-processing methods which involve wave polarizations, it seems likely that care in selection of receiver sites can alleviate this threat.

Finally, micropulsations do not originate from point sources, and consequently they are likely to display a certain degree of incoherence over a large sensor-array aperture. The degree to which the finite extent of micropulsation source regions will limit sensor-arraying techniques is also unknown, but if the reported source-region dimensions of several hundred kilometers (54) are correct, then arrays of a few hundred kilometers at thousands of kilometers distance from these sources should be useful.

It is our plan to attempt an investigation of the degree to which polarization diversity, sensor arraying, and multitype sensor comparison techniques can achieve the

improvements in noise rejection which appear to be possible. We wish to emphasize that, whereas some evidence exists to support each approach we have suggested, there has been to our knowledge no systematic, thorough investigation of the potential quantitative effectiveness of any of them. We propose simply to extend the study of these existing ideas to achieve that quantitative result.

Ionospheric Chemical Releases

A preliminary test of cesium-plasma-cloud deposition in the lower E region was conducted at NASA Wallops Station, Virginia, in March and April 1972. The objective of this test was threefold:

1. To field test the air-core induction antennas for the purpose of determining their sensitivity and suitability for use in remote sites under primitive conditions.
2. To perform a thoroughly instrumented study of cesium plasma clouds explosively deployed in the lower ionosphere and to verify the degree of their conformance to predictions.
3. To evaluate the sensor-arraying method for discerning a small, localized ionospheric-conductivity perturbation and, perhaps, a traveling ducted wave emitted from this localized disturbance.

It was not possible to design an experiment which would be optimum for all three objectives. For as thorough as possible knowledge of the interaction of the plasma cloud with the geomagnetic field (and incidentally with the lower ionospheric winds which may influence this interaction), it was necessary to photograph the plasma cloud from a set of precisely known sites so that triangulation could be used to describe the shape and motion of the growing cloud. Such photographic procedures can be conducted only during twilight, when the ionospheric currents are relatively weak and ionospheric conductivity is low. In view of the need for full knowledge of the behavior displayed by the plasma cloud, especially during the first 10 to 20 seconds of growth, it was decided to accept the less than optimum conditions available at twilight for this first test, in the interest of gaining direct information on cloud evolution. A second set of measurements under optimum conditions for interaction with the geomagnetic field are planned using knowledge gained from the preliminary experiment as a basis. The second experiment is tentatively planned for June or July 1973.

The March-April 1972 series consisted of four separate plasma-cloud launches and employed a number of different methods in an attempt to select optimum release height and payload composition. To fully investigate the entire dynamo region, releases were planned for four heights in the 90 to 140-km interval. Actual releases took place at 87, 106, 110, and 140 km.

The lowest altitude release was intended to investigate whether significant plasma-cloud interaction with the geomagnetic field could take place at the lower limit of the E region, where collisional processes involving ions and neutrals are expected to prevent substantial interaction. Details of this experiment will be presented elsewhere.

The highest altitude release was intended to explore the possibility, introduced in Part 2, that a plasma cloud above the dynamo region could act as a source of electromotive force and could drive a current through the highly conducting layer in the lower E region. The test succeeded in demonstrating that a large enough and dense enough plasma cloud can be created by explosive injection of cesium to permit this concept to be tested.

The third and fourth releases were intended to probe the portion of the dynamo region having the highest conductivity, namely that portion between 100 and 110 km. Two methods of plasma-cloud and deposition perturbation were employed. In one case a two-payload vehicle was launched, and it ejected the package of cesium salt plus high explosives ahead of a second cannister containing only high explosives. The objective in this experiment was to determine whether the additional thermal excitation of an explosion taking place within an already-deployed cloud could significantly increase the ionization. With the two-payload technique, a release-time separation of about 10 s was achieved, resulting in a release-point separation of about 1 km. No sudden increase in plasma-cloud charged-particle density was observed, however, and it is believed that the second explosion was too far from the region of high cesium density to cause discernible impulsive ionization.

In the second case a rocket containing a single payload of cesium plus high explosives was followed, after a 2-min delay, by a second rocket containing a payload comprising high explosives only. The objective of this test was to determine whether a simple sounding rocket of a type that is readily available and inexpensive to fly could be launched with adequate precision to hit the same point in space as that hit by an earlier identical vehicle. This test succeeded in exploding the second payload within 200 m of the plasma-cloud center and resulted in several pronounced effects on the plasma cloud. It will be discussed in greater detail in the following.

Instrumentation for this series of experiments was of several types:

1. Two K-46 ballistic cameras, with $f/2.5$ lenses and 5-in.-wide film, were placed at each of three sites suitably located for triangulation. One camera at each site was loaded with Kodak Type 2424 infrared-sensitive film (the principal cesium atomic emission line is in the infrared). The other camera was loaded with Kodak Royal X panchromatic film (the payload was lightly salted with sodium, whose principal atomic line is yellow, thus giving an indication to the naked eye of cloud shape and position). These cameras were automatically cycled through a sequence of 1.5-, 3.5-, and 8.5-s exposures.
2. Four Flight Research Model 370 70-mm cameras (a special design for NASA) with lens aperture settings of $f/1.0$ to $f/2.0$ were placed on a single mount at Wallops Station and automatically triggered simultaneously, with a 0.5-s exposure time per frame. Two of these cameras were loaded with Kodak Type 2424 film, one was loaded with Kodak Type 2485 film (sensitive to the visible spectrum), and another was loaded with Kodak Type 3443 infrared-sensitive color film. The objective of this photographic coverage was to obtain rapid-sequence photography of the developing plasma-cloud shape as viewed in a direction along the magnetic field.
3. A 13-MHz radar at Chesapeake Beach, Maryland, illuminated the releases and measured radar cross section, apparent plasma-cloud velocity, and internal motions of the plasma cloud. The objective of this measurement (see 4. below for an associated measurement) was to continuously monitor the apparent size of the

plasma cloud at the electron-density boundary of nominally $2 \times 10^6 \text{ cm}^{-3}$ and to discern the velocities and apparent sizes of prominent features which appeared in it. The angle of incidence on the plasma cloud from this radar site was about 40° from the direction of the magnetic field.

4. Four separate high-frequency radars were operated from Camp Lejeune, North Carolina, at frequencies of 7, 11, 17 and 28 MHz. These radars measured radar cross section, apparent plasma-cloud velocity, and internal motions of the plasma cloud from an aspect perpendicular to the magnetic-field direction. It was the objective of this experiment to obtain a complete record of plasma-cloud size at electron-density boundaries of nominally 6×10^5 , 1.5×10^6 , 3.6×10^6 , and 10^7 cm^{-3} . Particular attention was devoted to comparing these observations from an aspect transverse to the magnetic field with those from Chesapeake Beach, Maryland.
5. A 140-MHz radar at Chesapeake Beach, Maryland, illuminated the releases in an attempt to measure the behavior of the expanding plasma cloud at the electron-density boundary of $2.5 \times 10^8 \text{ cm}^{-3}$.
6. A 6- to 16-MHz ionospheric sounder was operated at NASA Wallops Station and measured peak electron density in the plasma cloud at late times, as well as apparent cloud size as viewed from along the magnetic-field direction.
7. A two-station network of air-core induction magnetometers, as described previously under Apparatus, was placed on a 300-km east-west baseline between Wallops Island and Buena Vista, Virginia. It was the intent of this network to discern any local magnetic perturbations which were generated by the plasma-cloud releases and to measure the propagation parameters of any ducted ULF waves which might have been launched by these perturbations. It must be emphasized that this preliminary experiment was intended principally to field test the apparatus and observing techniques and to gather vital diagnostic data on the plasma clouds. The tests were not conducted during the optimum time of day or season for the generation of geomagnetic perturbations, and the apparatus was still somewhat in the process of development and was not optimum for detecting small magnetic disturbances. (The results of this preliminary experiment have confirmed the value of the sensor-arraying method but have exposed several shortcomings of the air-core inductors, as we have stated previously under Apparatus. They also have led to an improvement in sensitivity, which we plan to exploit in subsequent experiments.)

The result of the radar and photographic measurements will be reported elsewhere. They succeeded in describing the dynamic behavior of explosively deployed cesium plasma clouds. In particular, the volume of space occupied by a plasma cloud of this type, the degree of ionization achieved, and the time scale of evolution of these parameters have all been documented. These results will make it possible to make improved estimates of the dynamics of plasma-cloud interaction with the geomagnetic field for the second series of experiments. The cloud sizes and charged-particle densities achieved and the time scale in which they grew confirm our expectation that significant interaction with the mid-morning or mid-afternoon summer ionosphere should be possible.

One result of the magnetometer measurements is worthy of mention here. The fourth cesium release created a plasma cloud of more than 10^7 charged particles/ cm^3 at an altitude of 106 km. Its volume was about $4 \times 10^9 \text{ m}^3$. (This is an approximate figure, because the volume was different for different charged-particle density contours—it was $5 \times 10^8 \text{ m}^3$ at the

10^7-cm^{-3} contour and $2.5 \times 10^{11} \text{ m}^3$ at the 10^6-cm^{-3} contour.) The second, high-explosives payload was exploded within 200 m of the plasma-cloud center and hence was burst within the 10^7-cm^{-3} contour. This second burst had an immediate pronounced effect on the radar cross section at the 10^7-cm^{-3} contour, but had no discernible effect on the outer contours. Thus its blast-wave effects were confined to the inner 500 m of the radius of the plasma cloud. Spectral data from the radar signal indicate that this perturbation was characterized by an extremely broadband, impulsive appearance, with a Doppler spectrum at least 20 Hz wide.

These facts are of vital importance for understanding a simultaneous signal which was obtained at the local magnetometer site (the Wallops Island site). A signal of about 10 mV appeared coincident with the second burst on both horizontal-axis sensors. It was of about 5 s duration and displayed a strong spectral component at about 10 Hz. This spectral component corresponds to the position of a sharp low-pass-filter skirt which is present in the receiving system to avoid aliasing difficulties in digital signal processing. The strength of the 10-Hz signal component indicates that a large impulsive signal, with frequency content wider than the receiving-system passband, occurred simultaneously with the high-explosives burst and radar-cross-section enhancement. This signal represents strong evidence that even under conditions of weak ambient-dynamo-current flow a large *local* disturbance can be created in the magnetic field by these means. No effect was discerned at the remote magnetometer site, but system sensitivity was low enough that a ducted wave would probably have been below the threshold of detectability.

This probable detection of the local magnetic perturbation from a cesium plasma cloud released in the dynamo region at twilight suggests that under optimum conditions of ionospheric current flow a disturbance as large as 100 mV might be observed at the surface of the earth. With an estimated 20-dB improvement in system sensitivity now being implemented, it should be possible to perform a conclusive test of the feasibility of this technique for the generation of ducted ULF waves. Accordingly, a second experiment is planned tentatively for the summer of 1973.

Ionospheric-Heating Experiments

Experiments in both E-region and F-region heating by radio waves have begun, and initial progress will be reported elsewhere.

Stimulation of Wave-Particle Interactions in the Magnetosphere

Methods by which injection of cold plasma into the magnetosphere to stimulate the condition of latent instability of the magnetospheric plasma and thus permit generation and amplification of ULF waves have been discussed in the prior sections and in the open literature (22). It was mentioned in the preceding that the injection of a few kilograms of lithium metal into the near-equatorial region could be achieved by exploding a shaped-charge payload of lithium and high explosives slightly above the collision-dominated region of the atmosphere. A height of a few hundred kilometers would be adequate to avoid substantial collisional dissipation of the lithium jet; this could be achieved with a relatively inexpensive rocket vehicle.

The Atomic Energy Commission Los Alamos Scientific Laboratories (LASL) have conducted a number of shaped-charge barium-ion ejection experiments and have perfected a means of emitting a jet of ionized barium along the geomagnetic field (55). The process

of adapting this technique to shaped-charge injection of lithium is underway at LASL. Preliminary plans have been made by LASL to establish a launch pad on the south island of New Zealand, as suggested above in Part 3 of this report, and negotiations by NRL for ULF sensor sites in New Zealand are in progress.

Stimulation of Wave-Wave Interactions in the Magnetosphere

A VLF transmitter is currently under construction by Stanford University at Siple, Antarctica, which has a geomagnetic L value of between 4 and 5. This location is a good one for the stimulated VLF emissions which it is intended to investigate and could be quite valuable as well for the stimulated ULF emissions which would result from a three-wave interaction as discussed before in Part 3 of this report. Use of the Stanford facility for a ULF stimulated-emission experiment would simply require appropriate modulation of the VLF transmitter.

It would be desirable to conduct at a lower geomagnetic latitude a complementary experiment employing a Navy VLF transmitter. Plans now are being formulated to conduct such an experiment within the next two years, with ULF sensors located in the vicinity of the transmitter (probably NAA) and if possible near the geomagnetic conjugate (which, for NAA, is in the Antarctic).

4. SUMMARY AND CONCLUSIONS

We have described a number of physical phenomena which occur naturally in the magnetosphere and ionosphere that may make it possible to use frequencies between 0.5 and 5 Hz for low-data-rate communications with deeply submerged submarines. A communications system employing this frequency band could not be conceived as a direct competitor to the SANGUINE ELF communications system but might represent a valuable supplement to the latter system under two circumstances. First, if future submerged-warfare technology requires communications from shore-based transmitters to receiving stations at several hundred meters depth, the ULF band will have an advantage of about 70 dB relative to the proposed ELF system in attenuation due to sea water. Second, under the conditions of geophysical variability which follow large solar eruptions and high-altitude nuclear explosions, communications via ELF may be significantly disturbed (56). Under these conditions, a ULF system may be capable of restoring partial communications.

Two general results from the study of natural geomagnetic phenomena have made it attractive to consider the ULF band as a candidate for a communications system. Geomagnetic micropulsations have been found to undergo a natural amplification process in the magnetosphere which it may be possible to exploit and which may provide up to 30-dB enhancement of signal amplitude. Furthermore, it has been found that micropulsations which impinge on the ionosphere after traversing this magnetospheric amplifying region then propagate in an ionospheric duct which is characterized by an attenuation rate as low as 1 to 2 dB/1000 km. It thus may be possible for electromagnetic energy to reach the surface of the earth over regions thousands of kilometers in extent with very low spreading loss.

With this motivation, we have embarked on a program to investigate whether these phenomena may be exploited by artificial excitation of ULF waves in the ionosphere and magnetosphere. Little is known of the natural mechanisms of micropulsation generation,

and so we have very limited evidence on which to base our effort. We have selected a number of candidate mechanisms which seem to involve the most likely means of stimulating the ionosphere and magnetosphere in the frequency band of interest. These means are divided into two basic approaches: (a) modulating the naturally flowing electric currents in the ionosphere and thus coupling energy into the magnetic field, and (b) driving the magnetospheric amplification region into a regenerative state and thus giving rise to micropulsation-like "oscillations," which may be controllable.

We have described two methods by which the former approach may be implemented. One of these methods involves the deposition of an ionized gas into the highly conducting region of the lower ionosphere. We have shown by calculations that this method, employing a few hundred pounds of cesium nitrate plus a high explosive, can cause a transient magnetic-field fluctuation of about 10 mγ/s on the surface of the earth below the disturbed ionospheric region. An initial experiment has shown that an effect of such magnitude can be produced by this means. Further experiments will be necessary to determine whether ducted ULF waves can also be generated by this method.

We have also described techniques by which RF heating of the ionosphere also causes modulation of the ionospheric electric currents. Calculations have indicated that magnetic-field fluctuations on the earth of several milligammas also can be stimulated by this means. Because a radio heating transmitter can be modulated at a controlled rate for arbitrarily long periods of time, coherent integration techniques can be used to enhance the geomagnetic field variations relative to noise and thus should permit high signal-to-noise ratios to be achieved.

We also have described two means by which the magnetospheric amplifying region might be caused to generate ULF waves. One such means involves the injection of an ionized gas into the magnetosphere at a distance of several earth radii above the equator, and the other one involves stimulation of a three-wave interaction by transmission of strong VLF pump and idler waves into the magnetosphere by a whistler mode. Both of these mechanisms involve nonlinear processes in the magnetosphere, and we have described them only qualitatively. We hope to attempt the detection of stimulated ULF emission from the injection of ionized lithium into the magnetosphere.

We have discussed the capabilities of state-of-art ULF sensing methods, and have concluded that induction sensors of the air-core and ferromagnetic-core types are adequate for some investigative purposes in our program. Capacitive sensors are less useful, but it seems attractive to develop a vertical-electric-field sensor for use in direction-finding and noise processing. Because most state-of-art ULF sensing systems have sensitivity limits very near the level of geomagnetic and atmospheric noise, it is also most attractive to develop a sensor of inherently higher sensitivity. Superconducting magnetometers which employ the Josephson Effect appear to be capable of providing at least 20 dB greater sensitivity than the best available induction systems.

We have described the general characteristics of ULF noise both from geomagnetic sources and from atmospheric discharges. A thorough investigation of the spatial and temporal correlative properties and of the polarization characteristics of this noise seems warranted.

REFERENCES

1. J.A. Jacobs, *Geomagnetic Micropulsations*, Springer-Verlag, New York, 1970.
2. V.A. Troitskaya and A.V. Gul'el'mi, "Geomagnetic Pulsations and Diagnostics of the Magnetosphere," *Sov. Phys. Uspekhi* 12, 195, (1969).
3. H.W. Smith, "Some Observations and Characteristics of Type Pc 1 Geomagnetic Micropulsations," *J. Geophys. Res.* 69, 1875 (1964).
4. J.A. Jacobs and T. Watanabe, "Theoretical Notes on Whistlers and Periodic Emissions in the Hydromagnetic Regime," *Planet. Space Sci.* 15, (1967).
5. R.R. Heacock, "The Relation of the Pc 1 Micropulsation Source Region to the Plasmasphere," *J. Geophys. Res.* 76, 100 (1971).
6. R.C. Wentworth, L. Tepley, and K.D. Amundsen, "Intra- and Interhemisphere Differences in Occurrence Times of Hydromagnetic Emissions," *J. Geophys. Res.* 71, 1492 (1966).
7. R.N. Manchester, "Correction of Pc 1 Micropulsations at Spaced Stations," *J. Geophys. Res.* 73, 3549 (1968).
8. R.N. Manchester, "Propagation of Hydromagnetic Emissions in the Ionospheric Duct," *Planet. Space Sci.* 18, 299 (1970).
9. W.H. Campbell, "Rapid Auroral Luminosity Fluctuations and Geomagnetic Field Pulsations," *J. Geophys. Res.* 75, 6182 (1970).
10. C.F. Kennel, and H.E. Petschek, "Limit on Stably Trapped Particle Fluxes," *J. Geophys. Res.* 71, 1499 (1966).
11. H.B. Liemohn, "Cyclotron-Resonance Amplification of VLF and ULF Whistlers," *J. Geophys. Res.* 72, 39 (1967).
12. D.R. Criswell, "Pc 1 Micropulsation Activity and Magnetospheric Amplification of 0.2- to 5.0-Hz Hydromagnetic Waves," *J. Geophys. Res.* 74, 205 (1969).
13. J.M. Cornwall, "Micropulsations and the Outer Radiation Zone," *J. Geophys. Res.* 71, 2185 (1966).
14. L. Tepley and R.K. Landshoff, "Waveguide Theory for Ionospheric Propagation of Hydromagnetic Emissions," *J. Geophys. Res.* 71, 1499 (1966).
15. R.N. Manchester, "Propagation of Pc 1 Micropulsations from High to Low Latitudes," *J. Geophys. Res.* 71, 3749 (1966).
16. C. Greifinger and P.S. Greifinger, "Theory of Hydromagnetic Propagation in the Ionospheric Waveguide," *J. Geophys. Res.* 73, 7473 (1968).
17. R.L. Dowden, "'Micropulsation Mode' Propagation in the Magnetosphere," *Planet. Space Sci.* 13, 761 (1965).
18. T. Obayashi, "Hydromagnetic Whistlers," *J. Geophys. Res.* 70, 1069 (1965).
19. C. Altman and E. Fijalkow, "Mechanism of Transmission of Hydromagnetic Waves Through the Earth's Lower Ionosphere," *Nature* 220, 53 (1968).
20. R.R. Heacock and V.P. Hessler, "Polarization Characteristics of Individual Elements in a Pc 1 Micropulsation Event," *Nature* 224, 895 (1969).
21. R.R. Heacock, "Micropulsation Pc-1 Phase and Polarization Comparisons Between College and Kotzebue, Alaska," *Ann. Geophys.* 26, 653 (1970).

22. N. Brice, "Harnessing the Energy in the Radiation Belts," *J. Geophys. Res.* **76**, 4698 (1971).
23. K.J. Harker and F.W. Crawford, "Nonlinear Interaction between Whistlers," *J. Geophys. Res.* **74**, 5029 (1969).
24. K.J. Harker and F.W. Crawford, "Parametric Wave Amplification and Mixing in the Ionosphere," *J. Geophys. Res.* **75**, 5459 (1970).
25. A.C. Fraser-Smith and K.R. Roxburgh, "Triggering of Hydromagnetic 'Whistlers' by Sferics," *Planet. Space Sci.* **17**, 1310 (1969).
26. N.W. Rosenberg, C.T. Best, F.P. Delgreco, M.M. Klein, M.A. Macleod, T.M. Noel, and W.K. Vickery, "AFCRL Barium Release Studies 1967," Project Secede Special Report No. 4, Air Force Cambridge Research Laboratories, Jan. 26, 1968.
27. N.W. Rosenberg and D. Golomb, "Generation and Properties of High-Altitude Chemical Plasma Clouds," in *Progress in Astronautics and Aeronautics, Vol. 12*, Academic Press, New York, 1963, p. 395.
28. J.R. Davis, "Decameter and Meter Wavelength Radar Studies of Artificial Plasma Clouds in the Lower Ionosphere; 2," *J. Geophys. Res.* **76**, 5292 (1971).
29. G.V. Groves, "Initial Expansion to Ambient Pressure of Chemical Explosive Releases in the Upper Atmosphere," *J. Geophys. Res.* **68**, 3033 (1963).
30. D.F. Martyn, "Electric Currents in the Ionosphere, III. Ionization drift Due to Winds and Electric Fields," *Phil. Trans. Roy. Soc.* **A246**, 306 (1953).
31. A.V. Gurevich, "Disturbance of the Ionosphere by Radio Waves," *Geomag. and Aeron.* **11**, 803 (1971).
32. G.A.M. King, "The Night-E Layer, in *Ionospheric Sporadic E*, in E.K. Smith, Jr., and S. Matsushita, editors, Pergamon Press, New York, 1962, p. 219.
33. R.L. Showen, "Artificial Heating of the Lower Ionosphere," *J. Geophys. Res.* **77**, 1923 (1972).
34. R.E. LeLevier, "Artificial Heating of the Ionosphere-Early Time Phenomena," *J. Geophys. Res.* **75**, 6419 (1970).
35. W.F. Utlaut, "An Ionospheric Modification Experiment Using Very High Power, High Frequency Transmission," *J. Geophys. Res.* **75**, 6402 (1970).
36. W.B. Hanson, "Structure of the Ionosphere," *Satellite Environment Handbook*, F.S. Johnson, editor, Stanford Univ. Press, Stanford, 1965, p. 21.
37. "COSPAR International Reference Atmosphere," North-Holland Publ., Amsterdam, 1965.
38. S. Chapman, "Survey of Geomagnetic Eclipse Phenomena," in *Solar Eclipses and the Ionosphere*, W.J.G. Beynon and G.M. Brown, editors, Pergamon Press, New York, 1956, p. 221.
39. D.T. Farley, B.B. Balsley, R.F. Woodman, and J.P. McClure, "Equatorial Spread F: Implications of VHF Radar Observations," *J. Geophys. Res.* **75**, 7199 (1970).
40. H. Rishbeth, "The F-layer Dynamo," *Planet-Space Sci.*, **19**, 263 (1971).
41. H. Rishbeth, "Polarization Fields Produced by Winds in The Equatorial F-Region," *Planet. Space Sci.* **19**, 357 (1971).

42. W.F. Utlaut, E.J. Violette, and A.K. Paul, "Some Ionosonde Observations of Ionosphere Modification by Very High Power, High Frequency Ground-Based Transmission," *J. Geophys. Res.* **75**, 6429 (1970).
43. W.E. Gordon, R. Showen, and H.C. Carlson, "Ionosphere Heating at Arecibo: First Tests," *J. Geophys. Res.* **76** 7808 (1971).
44. W. Stoffregen, "Electron Density Variation Observed in the E-Layer Below an Artificial Barium Cloud," *J. Atm. and Terres. Phys.* **32**, 171 (1970).
45. R.A. Helliwell, *Whistlers and Related Ionospheric Phenomena*, Stanford University Press, Stanford, 1965.
46. W.H. Campbell, "Induction Loop Antennas for Geomagnetic Field Variation Measurements," ESSA Technical Report ERL 123-ESL 6, June 1969.
47. T. Ogawa, Y. Tanaka, T. Miura, and M. Yasuhara, "Observations of Natural ELF and VLF Electromagnetic Noises by Using Ball Antennas," *J. Geomag. Geoelec.* **18**, 443 (1966).
48. J.E. Lokken, J.A. Shand, and C.S. Wright, "Some Characteristics of Electromagnetic Background Signals in the Vicinity of One Cycle per Second," *J. Geophys. Res.* **68**, 789 (1963).
49. J.A. Jacobs and T. Watanabe, "Micropulsation Whistlers," *J. Atmos. Terres. Phys.* **26**, 825 (1964).
50. L.N. Baranskiy, "Some Characteristics of the Polarization of Pc1 Pulsations Associated With Their Waveguide Propagation," *Geomag. and Aeron.* **10**, 86 (1970).
51. J.T. Weaver, "The Electromagnetic Field within a Discontinuous Conductor with Reference to Geomagnetic Micropulsations Near a Coastline," *Can. J. Phys.* **41**, 484 (1963).
52. H.J. Duffus, J.K. Kinnear, J.A. Shand, and C.S. Wright, "Spatial Variations in Geomagnetic Micropulsations," *Can. J. Phys.* **40**, 1133 (1962).
53. R.A. Santirocco and D.G. Parker, "The Polarization and Power Spectrums of Pc Micropulsations in Bermuda," *J. Geophys. Res.* **68**, 5545 (1963).
54. W.H. Campbell, "Low Attenuation of Hydromagnetic Waves in the Ionosphere and Implied Characteristics in the Magnetosphere for Pc 1 Events," *J. Geophys. Res.* **72**, 3429 (1967).
55. E.M. Wescott, H.M. Peek, H.C.S. Nielsen, W.B. Murcray, R.J. Jensen, and T.N. Davis, "Two Successful Geomagnetic-Field-Line Tracing Experiments," *J. Geophys. Res.* **77**, 2982 (1972).
56. J.R. Davis, E.L. Althouse, and D.R. Uffelman, "Some Possible Propagation-Associated Constraints on ELF Communications," NRL Report 7269, July 14, 1971.

DOCUMENT CONTROL DATA - R & D

(Security classification of title, body of abstract and indexing annotation must be entered when the overall report is classified)

1. ORIGINATING ACTIVITY (Corporate author) Naval Research Laboratory Washington, D.C. 20375		2a. REPORT SECURITY CLASSIFICATION UNCLASSIFIED	
		2b. GROUP	
3. REPORT TITLE MAGIC MODE: INVESTIGATIONS OF ARTIFICIAL STIMULATION OF ULF WAVES IN THE IONOSPHERE AND MAGNETOSPHERE			
4. DESCRIPTIVE NOTES (Type of report and inclusive dates) Final report on one phase of a continuing NRL problem.			
5. AUTHOR(S) (First name, middle initial, last name) John R. Davis, John W. Willis, and Edwin L. Althouse			
6. REPORT DATE March 12, 1973		7a. TOTAL NO. OF PAGES 48	7b. NO. OF REFS 56
6a. CONTRACT OR GRANT NO. NRL Problem R07-23		9a. ORIGINATOR'S REPORT NUMBER(S) NRL REPORT 7552	
b. PROJECT NO. RF 21-222-401 and RF 21-222-402		9b. OTHER REPORT NO(S) (Any other numbers that may be assigned this report)	
c.			
d.			
10. DISTRIBUTION STATEMENT Approved for public release; distribution unlimited.			
11. SUPPLEMENTARY NOTES		12. SPONSORING MILITARY ACTIVITY Department of the Navy Office of Naval Research Arlington, Virginia 22217	
13. ABSTRACT <p>This report describes an investigation of the potential usefulness of the ultra-low-frequency (ULF) band for communications with deeply submerged reception terminals. The discussion begins with a comprehensive review of present knowledge about ULF propagation. Present understanding of ULF propagation modes (based on observations of naturally occurring geomagnetic micropulsations) is summarized, and those features which are of importance to potential communications systems are discussed.</p> <p>Emphasis is then placed on the study of potential ULF generation mechanisms between 0.2 and 5 Hz which would benefit from the naturally occurring magnetospheric amplification process that is observed to occur in that frequency band. Two possible source regions are considered for the artificial generation of ULF waves: the ionospheric dynamo and the magnetospheric proton belt. Several means are postulated for manipulating the parameters in these regions so as to stimulate artificial micropulsations; among them are a three-wave VLF-ULF interaction in the magnetosphere, lithium-plasma injection into the trapped-proton belt of the magnetosphere, deposition of highly ionized plasma clouds in the ionospheric dynamo, and modification of dynamo electron densities via high-powered, high-frequency radio waves. The latter two methods are judged most attractive and are treated quantitatively. The principal means of detecting signals in the ULF frequency range are described, citing the advantages and disadvantages of the various instruments. The preliminary results of a long-term experimental investigation in this area are discussed, including a description of future experiments designed to explore the concepts contained in this report.</p>			

14. KEY WORDS	LINK A		LINK B		LINK C	
	ROLE	WT	ROLE	WT	ROLE	WT
ULF Communications to submerged vehicles Magnetosphere Magnetospheric ion injection Plasma cloud Ionospheric heating VLF wave interaction Micropulsations Geomagnetic variations Magnetic field sensors						